

ERDC/EL TR-04-17

Environmental Laboratory



**US Army Corps
of Engineers®**
Engineer Research and
Development Center

Environmental Restoration Research Program

Xenon Spectral Gamma Penetrometer Probe Characterization and Calibration

John H. Ballard, Charles A. Sparrow, and John C. Morgan

September 2004

Xenon Spectral Gamma Penetrometer Probe Characterization and Calibration

John H. Ballard and John C. Morgan

*Environmental Laboratory
U.S. Army Engineer Research and Development Center
3909 Halls Ferry Road
Vicksburg, MS 39180-6199*

Charles A. Sparrow

*Dave C. Swalm School of Chemical Engineering
P.O. Box 9595
Mississippi State University
Mississippi State, MS 39762-9595*

Final report

Approved for public release; distribution is unlimited

Prepared for	U.S. Department of Energy, National Energy Technology Laboratory 3610 Collins Ferry Road, Morgantown, WV 26507-0880
Under	DOE NETL Task 007
Monitored by	U.S. Army Engineer District, Pittsburgh William S. Moorhead Federal Building 1000 Liberty Avenue, Pittsburgh, PA 15222-4186

ABSTRACT:

Ex situ analysis to characterize subsurface media for gamma-emitting radionuclides is time-consuming and costly. A Site Characterization and Analysis Penetrometer System (SCAPS) spectral gamma penetrometer probe was designed using newly developed small-diameter high-pressure xenon gas gamma ray detector technology for the in situ speciation (identification) and quantification of subsurface gamma-emitting contaminants. This report documents the design, calibration, laboratory studies, and functionality field demonstration conducted to characterize the capabilities and limitations of the xenon spectral gamma probe. Results and comparative analysis of side-by-side simultaneous laboratory investigation/evaluation studies using SCAPS xenon spectral gamma and sodium iodine spectral gamma probes are also documented.

DISCLAIMER: The contents of this report are not to be used for advertising, publication, or promotional purposes. Citation of trade names does not constitute an official endorsement or approval of the use of such commercial products. All product names and trademarks cited are the property of their respective owners. The findings of this report are not to be construed as an official Department of the Army position unless so designated by other authorized documents.

Contents

Preface	vii
1—Introduction	1
2—SCAPS Xenon Spectral Gamma Penetrometer Probe Components	3
Xenon Gas Gamma Detector/Preamplifier Assembly	3
Probe Components	3
Umbilical Cable Components	6
3—Detector Laboratory Evaluation Studies	9
Laboratory Radiological Background Minimization	9
Effects of Vibration-Induced Electronic Noise	9
Spectral Resolution Verification Study	13
4—Xenon Probe Calibration	17
Calibration Isotopes	17
Calibration Media Preparation	17
Xenon Gas Spectral Gamma Probe Calibration	18
Calibration Documentation	19
Correction for semi-infinite medium	22
Calculation of calibration coefficient	22
5—Xenon Probe/Sodium Iodide Probe Comparison	26
Laboratory Comparison in Calibration Media	26
Resolution Verification	28
6—Functionality Field Demonstration	30
Pre-Demonstration Field Evaluation	30
Functionality Demonstration Site Configuration	30
Continuous-Push Data Acquisition	32
Stationary-Mode Data Acquisition	32
7—Conclusions	36
8—Recommendations	37
References	38
SF 298	

List of Figures

Figure 1.	Mirmar-developed high-pressure xenon gas gamma detector/preamplifier assembly	4
Figure 2.	Mirmar-developed xenon gas gamma detector preamplifier	4
Figure 3.	SCAPS xenon gas spectral gamma probe configuration	5
Figure 4.	Xenon gas gamma detector probe housing design drawings	6
Figure 5.	Xenon gas gamma detector probe adapter for a soil classification module	7
Figure 6.	Xenon gas gamma detector probe adapter for commercial push rods.....	7
Figure 7.	Umbilical cable configuration for the xenon spectral gamma/soil classification probe	8
Figure 8.	Laboratory configuration of xenon and sodium iodide spectral gamma probes with lead brick shielding, Mississippi State University Radiological Laboratory	10
Figure 9.	Xenon gas gamma detector logarithmic energy spectrum of naturally occurring laboratory background radiation without vibration isolation	10
Figure 10.	Xenon gas gamma detector logarithmic energy spectrum of naturally occurring laboratory background radiation with vibration isolation.....	11
Figure 11.	Xenon gas gamma detector logarithmic energy spectrum of vibration-induced electronic noise	12
Figure 12.	Xenon gas gamma detector linear energy spectrum of vibration-induced electronic noise	12
Figure 13.	Xenon gas gamma detector energy spectrum of 1 μ Ci Cs-137 and 1 μ Ci Co-60 laboratory sources	13
Figure 14.	Calibration disk designed by Mississippi State University using thorium-232 with progeny in equilibrium	14
Figure 15.	Xenon gas gamma detector energy spectrum collected over the Mississippi State University 50 pCi/g thorium-232/thorium progeny calibration disk	15

Figure 16.	Sodium iodide gamma detector with lead ring positioned 10 cm above the Mississippi State University 50-pCi/g thorium-232/thorium progeny calibration disk	15
Figure 17.	Sodium iodide gamma detector energy spectrum collected over the Mississippi State University 50-pCi/g thorium-232/thorium progeny calibration disk	16
Figure 18.	Xenon gas gamma detector energy spectrum collected over the Mississippi State University 50-pCi/g thorium-232/thorium progeny calibration disk	16
Figure 19.	Xenon gas spectral gamma probe inserted in calibration medium at the Mississippi State University Radiological Sensor Calibration Facility	18
Figure 20.	Nuclear instrument module data acquisition and processing system equipment used during probe calibration at the Mississippi State University Radiological Sensor Calibration Facility	19
Figure 21.	Geometry for distributed source	20
Figure 22.	Sodium iodide spectral gamma probe logarithmic energy spectrum collected with the probe surrounded by 18.3 cm of radioisotope-spiked soil medium	27
Figure 23.	Xenon gas spectral gamma probe logarithmic energy spectrum collected with the probe surrounded by 18.3 cm of radioisotope-spiked soil medium	27
Figure 24.	Xenon gas spectral gamma probe energy spectrum for 1 μ Ci Cs-137 and 1 μ Ci cobalt-60 laboratory sources	29
Figure 25.	Sodium iodide spectral gamma probe energy spectrum for 1 μ Ci Cs-137 and 1 μ Ci cobalt-60 laboratory calibration sources	29
Figure 26.	Cs-137 energy spectrum collected with the high-pressure xenon gas spectral gamma probe after baking	31
Figure 27.	Functionality demonstration site configuration used to evaluate the SCAPS high-pressure xenon gas spectral gamma probe in subsurface media	31
Figure 28.	Continuous xenon spectral gamma probe energy spectrum collected as the probe was push parallel to the tethered Cs-137 source at approximately 1.5 m depth	32
Figure 29.	Xenon gas spectral gamma probe logarithmic energy spectrum of two 1- μ Ci Cs-137 sources collected at a depth of 1.5 m through 15 cm of soil	33

Figure 30.	Xenon gas spectral gamma probe logarithmic energy spectrum of two 1- μ Ci Cs-137 sources collected at a depth of 1.5 m through 15 cm of soil	34
Figure 31.	Xenon gas spectral gamma probe energy spectrum of clean soil acquired at a depth of 13.71 m	35
Figure 32.	Xenon gas spectral gamma probe energy spectrum of two 1- μ Ci Cs-137 sources collected at a depth of 1.5 m through 15 cm of soil	35

List of Tables

Table 1.	Xenon Gas Spectral Gamma/Soil Classification Probe Umbilical Cable Components	8
Table 2.	Isotopes Used in Calibration Standard	17
Table 3.	Calibration Coefficient Ratios	24
Table 4.	Calibration Factor Summary	25
Table 5.	Calculated Xe and NaI Areas and Isotope Concentrations	28

Preface

This study was performed from October 1998 through September 2003 by the U.S. Army Engineer Research and Development Center (ERDC), Environmental Laboratory (EL), in support of the U.S. Department of Energy (DOE) National Energy Technology Laboratory (NETL) Task 007, Statement of Work entitled, "WES Support for the Design, Fabrication, Calibration, and Field Demonstration of the Enhanced Spectral Gamma Detection System Using Xenon Detector Technology for Site Characterization and Analysis Penetrometer System (SCAPS) Application." Mr. Ron Staubly was DOE-NETL Program Manager during the execution of this project.

The Program Manager and Principal Investigator for SCAPS Radiological Sensor Technology Application and Evaluation was Mr. John H. Ballard, ERDC, EL, Environmental Restoration Program Management Office (EM-J). Dr. M. John Cullinane, ERDC, EL, EM-J, was Technical Director for Environmental Engineering and Cleanup during this work. Mr. John C. Morgan, ERDC, EL, formerly of Alion Science and Technology, provided nuclear physics support during Mississippi State University (MSU) xenon gamma sensor calibration and laboratory investigations.

Dr. Charles A. Sparrow, MSU, provided nuclear engineering technical support during radiological laboratory investigations and during the calibration of the SCAPS Xenon Spectral Gamma Probe. Mr. Dan Y. Eng, ERDC, Information Technology Laboratory, Engineering and Informatic Systems Division, Automated Measurements and Analysis Branch, designed and oversaw the fabrication of SCAPS probe and umbilical cable components. Dr. Albert G. Beyerle, Mirmar Sensor, LLC, provided technical support during laboratory and functionality field investigations.

At the time of publication of this report, Dr. Beth C. Fleming was Acting Director, EL, and Dr. James R. Houston was Director of ERDC. Commander and Executive Director of ERDC was COL James R. Rowan, EN.

1 Introduction

The U.S. Army Engineer Research and Development Center (ERDC), part of which was formerly known as the Waterways Experiment Station (WES), designed, fabricated, calibrated, and evaluated the first Site Characterization and Analysis Penetrometer System (SCAPS) sodium iodide (NaI) spectral gamma penetrometer probe system in 1996 in support of the Department of Energy (DOE) EM-50, Office of Science and Technology. A SCAPS NaI spectral gamma probe was successfully demonstrated at the DOE Savannah River Site, South Carolina, R-Reactor Seepage Basin in 1997 (Argonne National Laboratory 1997; Morgan et al. 1997). The DOE documented savings of more than \$800,000 using the SCAPS in situ penetrometer interrogation system over conventional sampling technologies during the Savannah River Site SCAPS Spectral Gamma Technology Demonstration (Morgan et al. 1998).

ERDC, in support of the DOE Hanford Facility, designed and developed a SCAPS multisensor penetrometer probe for the simultaneous detection of gamma-emitting radionuclides, heavy metals, depth, and soil classification. The multisensor probe included a NaI spectral gamma detection and speciation system, an isotopic excited x-ray fluorescence (XRF) metals speciation system, a depth meter, and soil classification sensors that provided co-located gamma, metals, soil classification, and depth data (Ballard and Cullinane 1998).

ERDC, in support of the DOE National Energy Technology Laboratory (NETL), formerly the Federal Energy Technology Center (FETC), designed, fabricated, calibrated, and evaluated the first high-pressure xenon (Xe) gas spectral gamma penetrometer probe for SCAPS direct-push field applications. A newly developed small-diameter, high-pressure xenon gas gamma detector, manufactured by Mirmar Sensor, Inc., was selected for integration in a SCAPS penetrometer probe with soil classification sensors. The multisensor technology has the capability to conduct in situ subsurface analysis of gamma activity co-located with soil classification, depth, and soil layering data (Ballard et al. 2000, 2001).

ERDC designed and fabricated a special penetrometer probe housing and interface components to accommodate the dimensions of a small-diameter Mirmar xenon gas gamma detector/preamplifier assembly. The probe/detector assembly was integrated with a standard-configuration soil classification module and umbilical cable. Spectral gamma detector calibration and laboratory evaluation studies were conducted at the Mississippi State University (MSU) Radiological Sensor Calibration Facility, Starkville, Mississippi. Personnel of the ERDC, MSU, and Alion Science and Technology (ERDC on-site contract

employees) conducted laboratory evaluation and calibration experiments using unique MSU-developed gamma-emitting radionuclide calibration sources. The functionality field evaluation reported herein was conducted at the ERDC, Vicksburg, Mississippi, using the ERDC 20-ton SCAPS research truck to document the capabilities and functionality of the xenon spectral gamma probe to detect and speciate gamma activity in subsurface soil media in situ. The probe was operated in stationary and continuous-push modes.

This report documents the design and fabrication of the xenon spectral gamma probe, ERDC laboratory evaluation experiments, MSU calibration procedures and results, ERDC functionality field evaluation, and operational procedures and results.

2 SCAPS Xenon Spectral Gamma Penetrometer Probe Components

Xenon Gas Gamma Detector/Preamplifier Assembly

Mirmar Sensor, LLC, developed a unique gamma detection technology for cone penetrometer deployment. The Mirmar high-pressure xenon gas gamma detector/preamplifier assembly (Figure 1) is housed in a stainless steel cylinder measuring 4.45 cm in diameter \times 33.02 cm long (Figure 2). The sealed gas chamber has an active volume of 131.5 cm³ (4.06 cm diameter \times 10.16 cm long). The gas chamber contains an internal electrically isolated grid and acts as an ionization chamber. The gas chamber is evacuated and filled with a gas mixture containing 99.7 percent (high purity) xenon gas plus 0.3 percent hydrogen gas. The density of the gas mixture is 0.5 g/cm³. The outer surface of the cylinder is wrapped with an isolated conducting surface and forms a capacitor when high voltage is applied to the internal grid. The high-purity xenon gas acts as an ionization medium that reacts when gamma ray energy enters the high-pressure gas chamber. Spectral gamma energies are detected via the ionization of xenon gas particles, and the ionized energy is captured by the grid and transferred electronically via the preamplifier for spectral energy analysis. Thus the Mirmar xenon gas gamma detection system has the capability to capture unique gamma-emitting radionuclide emissions and to speciate (identify) multiple gamma emissions simultaneously using conventional nuclear instrument module (NIM) equipment and energy spectrum analysis techniques.

Probe Components

ERDC designed and fabricated SCAPS penetrometer probe components to accommodate the dimensions of the SCAPS truck's hydraulic chuck mechanism and the dimensions of the Mirmar xenon gas gamma detector/preamplifier assembly. A concept drawing of the SCAPS spectral gamma probe with soil classification sensors and SCAPS truck-mounted NIM data acquisition and processing system equipment is provided in Figure 3. The probe housing and interface components were fabricated in the ERDC machine shop from solid-stock

6.35-cm- (2.5-in.-) diameter H-13 tool steel bars. The probe housing was designed with 6.033-cm (2.375-in.) outside diameter (OD) dimensions and with 0.64-cm- (0.25-in.-) thick walls (Figure 4).

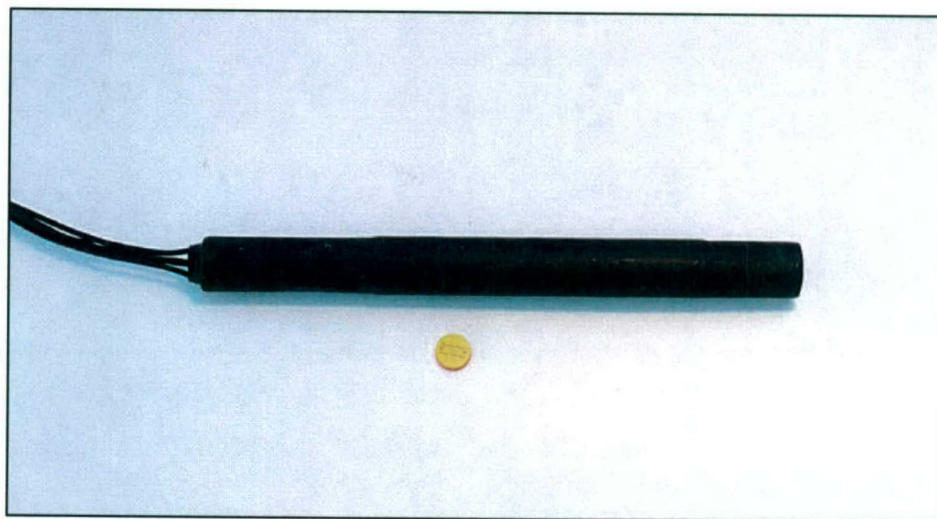


Figure 1. Mirmar-developed high-pressure xenon gas gamma detector/ preamplifier assembly (photo by Mirmar Sensor, LLC)

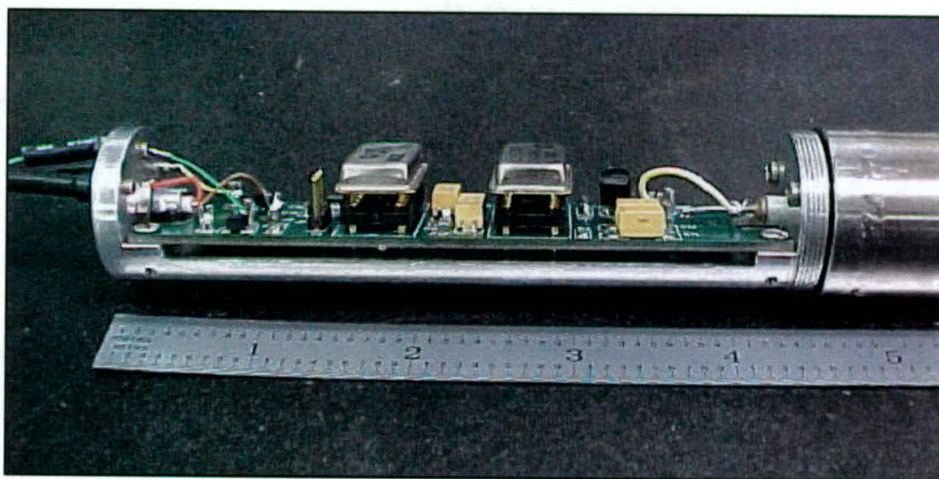


Figure 2. Mirmar-developed xenon gas gamma detector preamplifier (photo by Mirmar Sensor, LLC)

The wall thickness of the probe housing was optimized to enhance the durability of the probe, to maximize gamma ray penetration through the probe steel housing, and to accommodate the OD of the Mirmar gamma detector. A thicker wall dimension would have been desirable but would have increased the attenuation of incident gamma rays.

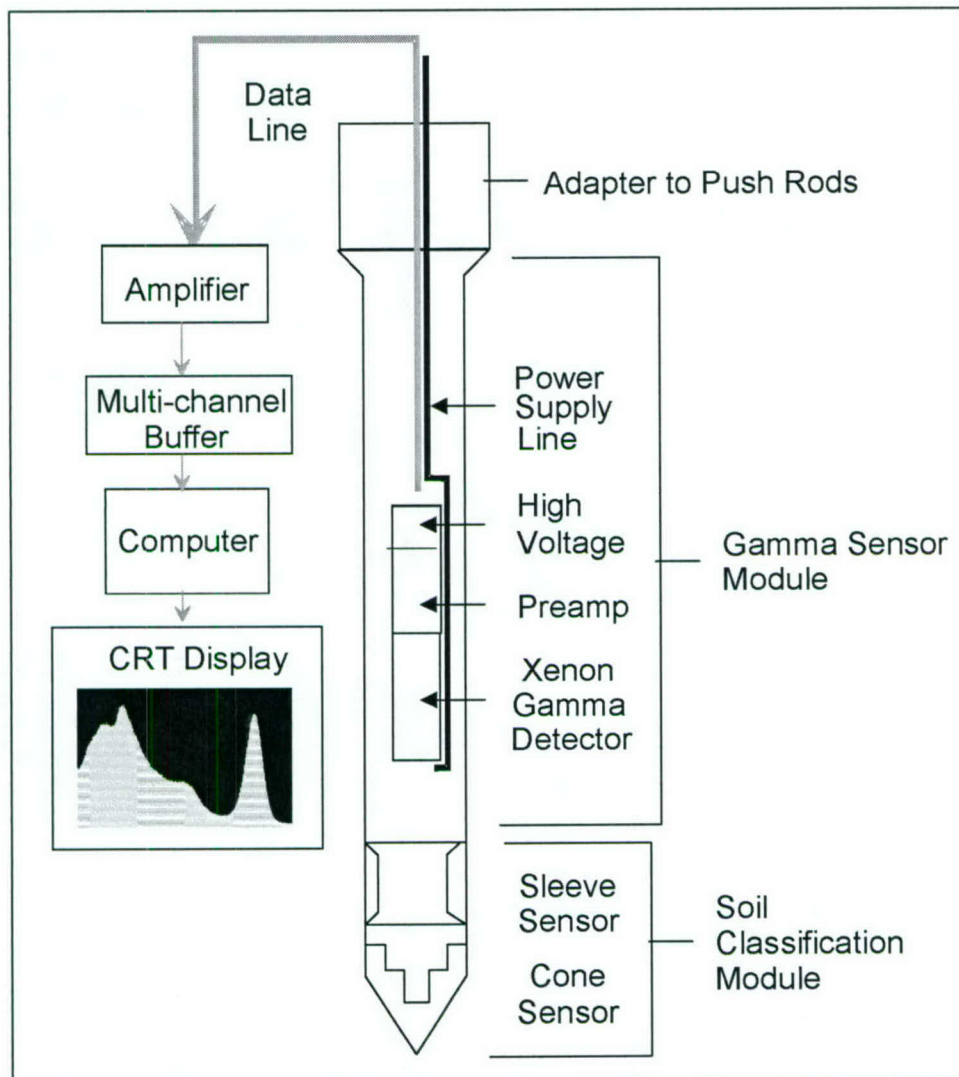


Figure 3. SCAPS xenon gas spectral gamma probe configuration

Probe components were fabricated to interface to a commercial 5.08-cm- (2-in.-) OD soil classification module (Figure 5) and to standard 4.45-cm- (1.75-in.-) OD penetrometer push rods (Figure 6). The steel probe housing and interface components were fabricated from solid H-13 steel rods. After fabrication, the steel probe components underwent commercial heat treatment and were hardened to 45-49 RC (Rockwell hardness). Probe components were hardened (heat treated) to provide added abrasion resistance and strength to the probe. The steel hardening process minimizes abrasive-induced scarring of probe surfaces that could become contaminated with radioactive subsurface soil.

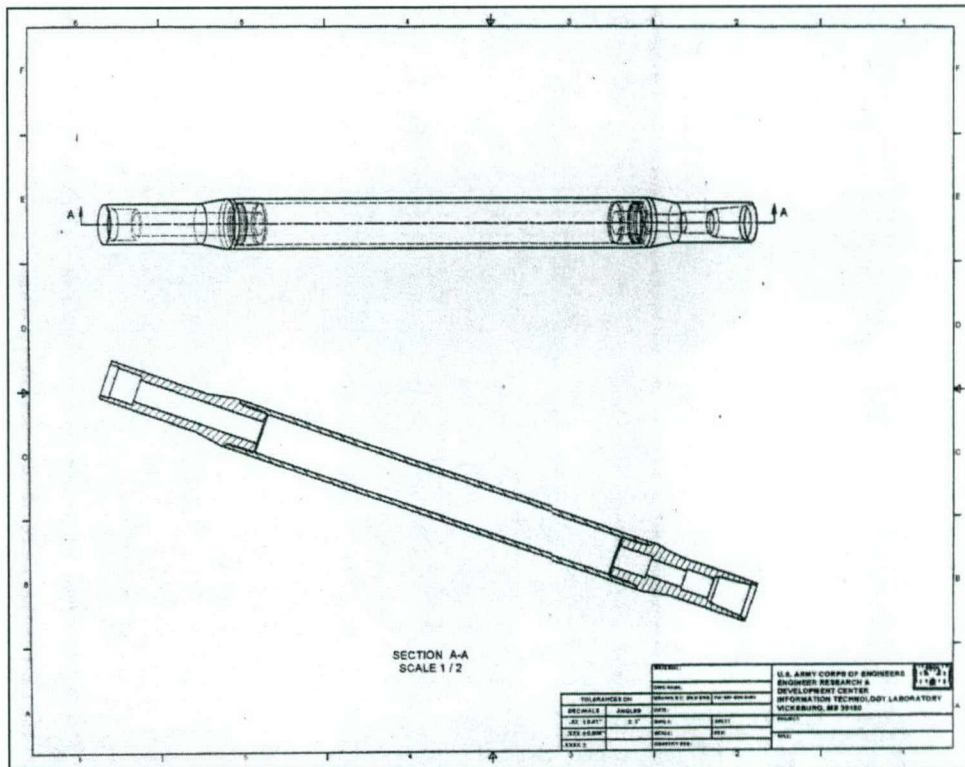
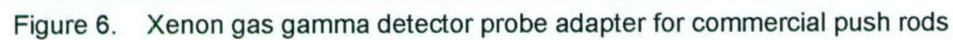
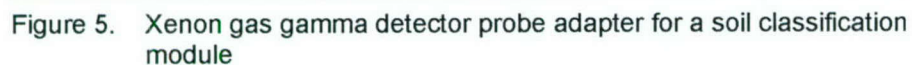


Figure 4. Xenon gas gamma detector probe housing design drawings

Umbilical Cable Components

The ERDC designed a SCAPS umbilical cable to interface subsurface spectral gamma and soil classification components with surface-mounted electrical power and data acquisition/processing equipment. The umbilical cable is deployed through hollow push rods that are used to hydraulically advance the spectral gamma penetrometer probe into subsurface media. The umbilical cable is approximately 50 m in length and is made up of 17 independently isolated data and power transmission lines plus one drain wire (for static electricity grounding) and is covered with a black polyurethane outer jacket with a minimum thickness of 0.13 cm (0.05 in.). The total diameter of the umbilical cable is approximately 1.43 cm (0.5625 in.) (Figure 7). The number-coded umbilical cable transmission lines are described in Table 1.



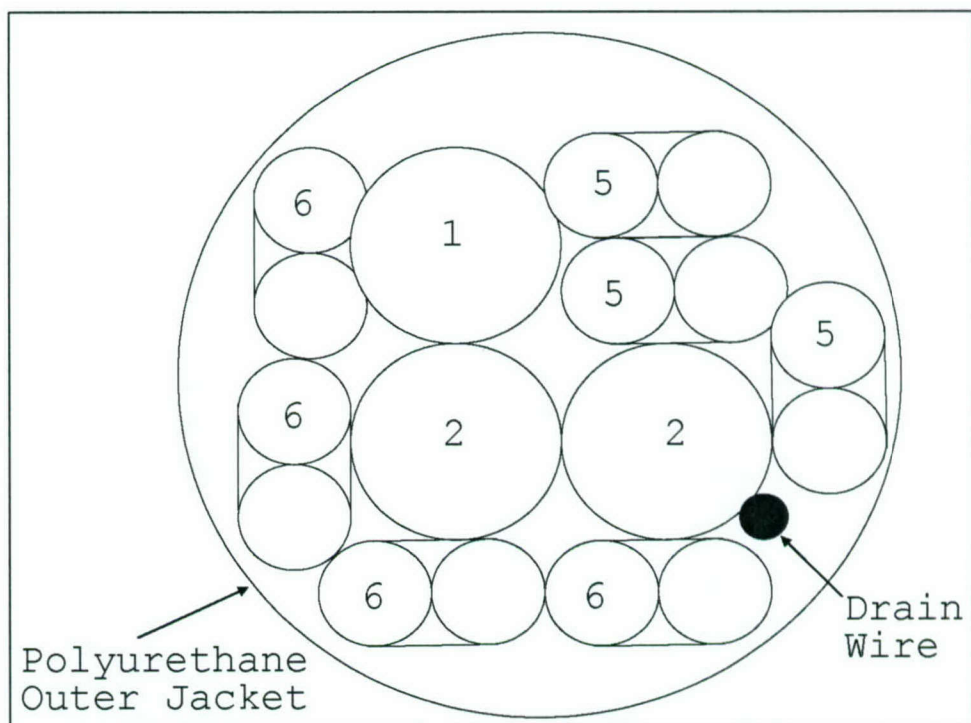


Figure 7. Umbilical cable configuration for the xenon spectral gamma/soil classification probe

Table 1 Xenon Gas Spectral Gamma/Soil Classification Probe Umbilical Cable Components	
Component No.	Transmission Line Color and Type
Xenon Gas Spectral Gamma Detection Module	
2	Reynolds P/N 167-2896, 5-kV high-voltage cable, 0.095-in. diameter (white)
2	Reynolds P/N 167-2896, 1- to 2-kV high-voltage cable, 0.095-in. diameter (white)
1	Belden P/N 84316 50-ohm coaxial signal cable, 0.098-in. diameter (brown)
5	+/- 6-V, 26 AWG shielded twisted pair (blue/white)
5	Ground and common, 26 AWG shielded twisted pair (blue/black)
5	Spare, 26 AWG shielded twisted pair (blue/green)
Soil Classification Module	
6	26 AWG shielded twisted pair (red/black)
6	26 AWG shielded twisted pair (black/white)
6	26 AWG shielded twisted pair (green/white)
6	26 AWG shielded twisted pair (green/red)

3 Detector Laboratory Evaluation Studies

Laboratory evaluation investigations and checkout experiments were conducted by ERDC at the MSU Calibration Facility to determine the functionality and response characteristics of the Mirmar xenon gas gamma detector. The Mirmar gamma detector was studied with and without the steel probe housing.

Laboratory Radiological Background Minimization

Laboratory investigations were conducted to determine the performance characteristics of the Mirmar small-diameter xenon gas gamma detector before and after the detector was installed in a steel penetrometer housing. Laboratory experiments were conducted with 2-in.-thick lead bricks placed beneath and to each side of the detector to minimize background radiation. The laboratory configuration for these investigations was similar to the xenon and sodium iodide spectral gamma probes configuration shown in Figure 8. Gamma energy spectra of background radiation were collected for each laboratory configuration and were used to strip naturally occurring radioactive background from radionuclide gamma energy spectra.

Effects of Vibration-Induced Electronic Noise

During laboratory investigations, it was noted that vibration appeared to induce electronic noise into the spectral signature generated by the xenon gas gamma detector. Natural building vibration was attributed to air conditioning and positive air pressure that was maintained in the laboratory. Background radiation was measured using the Mirmar xenon gas gamma detector in two configurations: (1) configuration 1 - detector response measured without vibration isolation; and (2) configuration 2 - detector response measured with vibration isolation. In each configuration, gross gamma activity and gamma energy spectral data were collected for 3600 seconds.

The Mirmar gamma detector in configuration 1 was positioned directly on lead bricks that were lying on a standard laboratory bench surface. Vibration isolation material was not used to minimize vibration-induced electronic noise. In

this configuration, the background produced 217,377 counts of gamma activity and produced the logarithmic gamma energy spectrum presented in Figure 9.

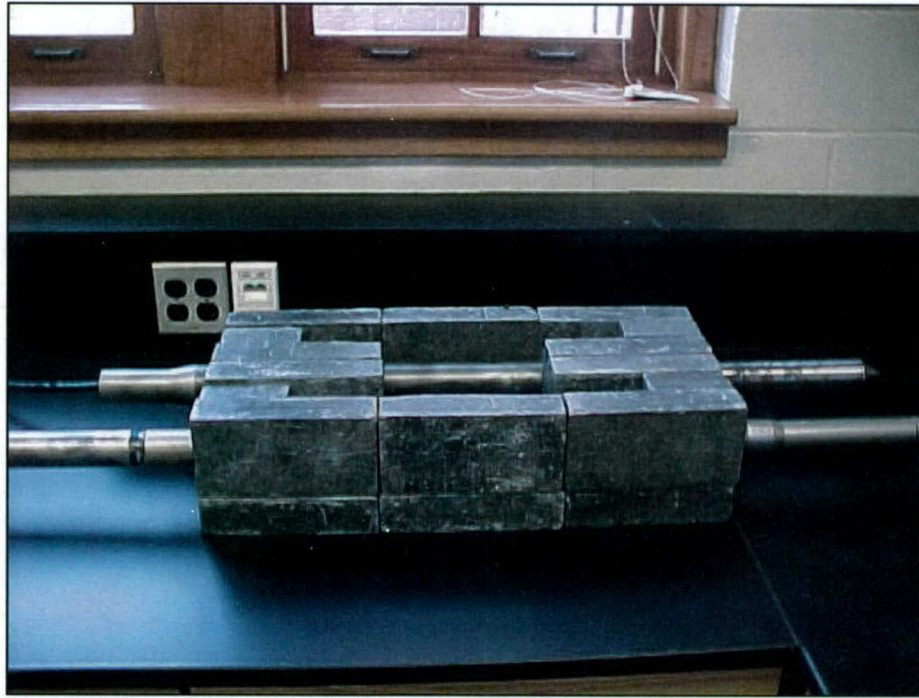


Figure 8. Laboratory configuration of xenon (rear probe) and sodium iodide spectral gamma probes with lead brick shielding, Mississippi State University Radiological Laboratory

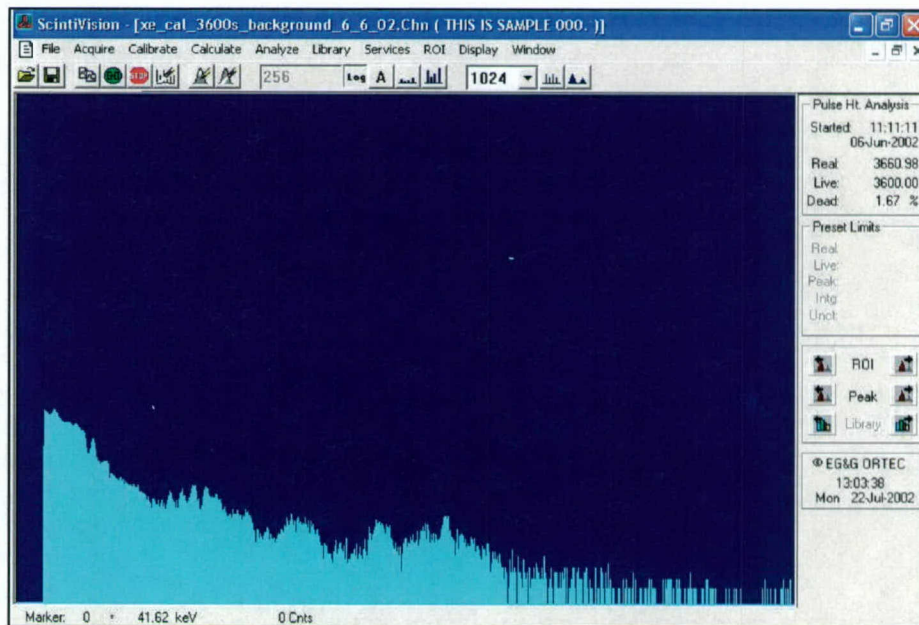


Figure 9. Xenon gas gamma detector logarithmic energy spectrum of naturally occurring laboratory background radiation without vibration isolation

The Mirmar gamma detector in configuration 2 was positioned on 2.54-cm-thick foam packing material and placed in the lead-shielded laboratory bench setup of configuration 1. In this vibration-minimized configuration, the background radiation produced 17,481 counts of gamma activity and produced the logarithmic nuclear energy spectrum in Figure 10. The use of vibration isolation material resulted in a 92-percent reduction in gross gamma activity counts. The difference in gross counts of gamma activity is equivalent to vibration-induced electronic noise. The results of this experiment verified that vibration-induced signals are introduced into spectral data and may produce a pseudo-spectrum of gamma activity. A resulting pseudo gamma spectrum was produced by stripping (subtracting) the spectrum of Figure 10 from Figure 9 and is presented in logarithmic and linear displays in Figures 11 and 12, respectively.

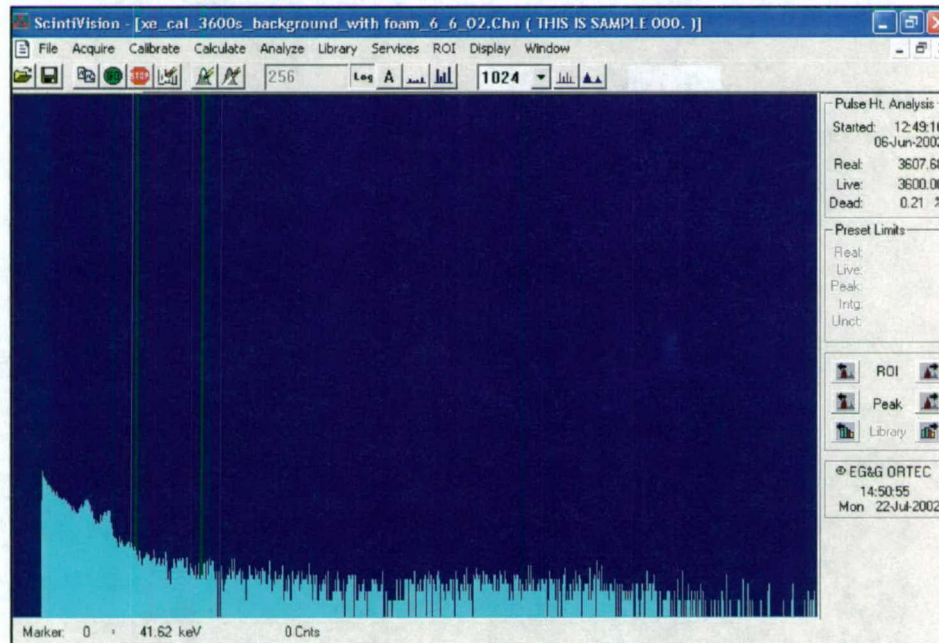


Figure 10. Xenon gas gamma detector logarithmic energy spectrum of naturally occurring laboratory background radiation with vibration isolation

Based on the results of these background laboratory investigations, vibration-induced electronic noise may be produced for some modes of SCAPS penetrometer truck deployment of the gridded xenon gas gamma detector. The amplitude of electronic noise is expected to vary with changes in subsurface soil media. Induced electronic noise is also likely to occur during continuous-push gamma detector field deployment activities. However, minimal vibration-induced electronic noise is expected when the probe is stationary and is conducting spectral gamma data collection activities. A study to determine the range of vibration-induced electronic noise for varying soil media and the effects on xenon gas gamma detector performance is beyond the scope of this project.

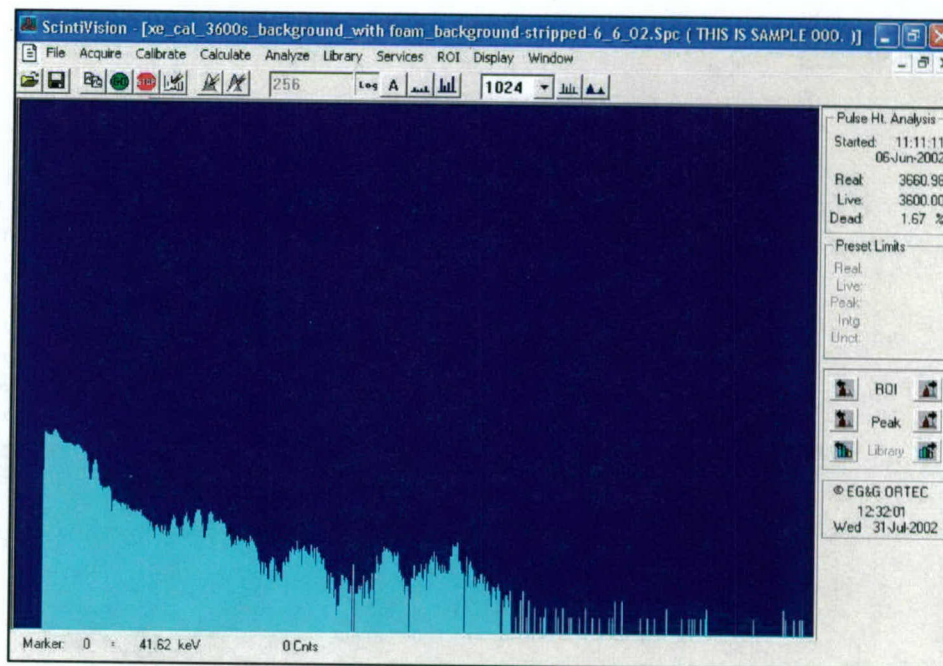


Figure 11. Xenon gas gamma detector logarithmic energy spectrum of vibration-induced electronic noise

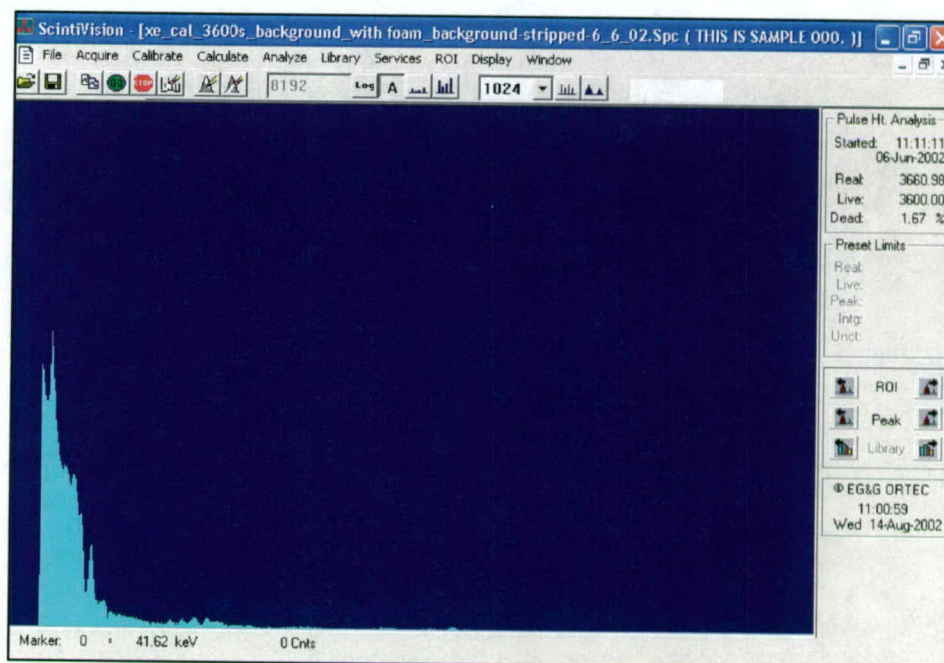


Figure 12. Xenon gas gamma detector linear energy spectrum of vibration-induced electronic noise

Spectral Resolution Verification Study

Laboratory investigations were conducted to determine the spectral resolution of the Mirmar xenon gas gamma detector/preamplifier assembly. The Mirmar detector was placed within the lead brick background minimization chamber described above. During the laboratory evaluation/checkout experiment, 1- μ Ci calibration sources of Cs-137 and Co-60 were placed 10 cm from the active portion of the xenon gamma detector ionization chamber of the Mirmar gamma detector. The Mirmar small-diameter gamma detector provided approximately 2.45-percent resolution for the 661.62-keV spectral energy line of Cs-137 and 1.6-percent resolution for the 1332.50-keV spectral energy line of Co-60. A gamma energy spectrum produced during the spectral resolution experiment is presented in Figure 13.

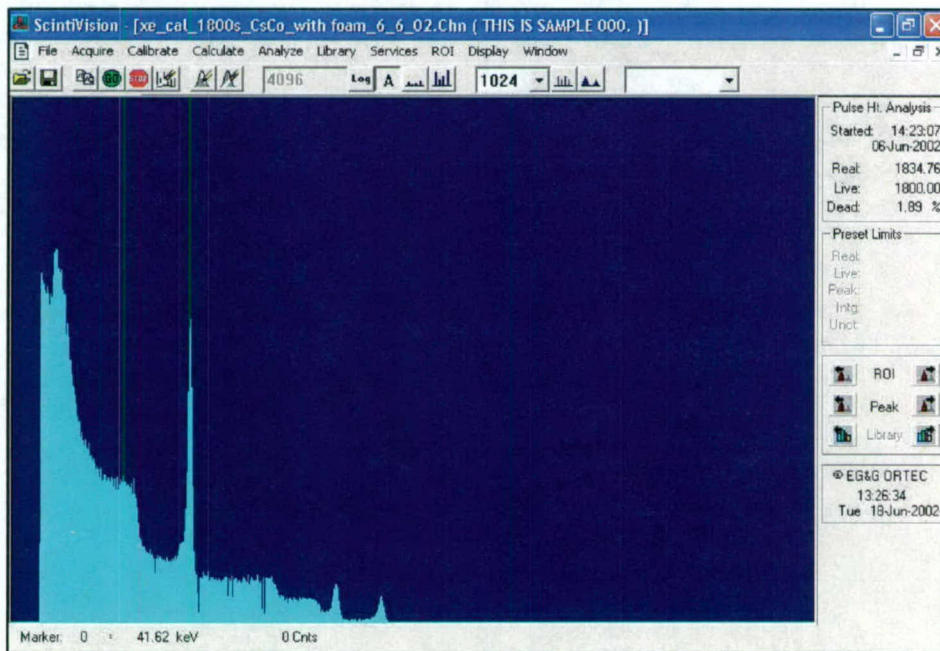


Figure 13. Xenon gas gamma detector energy spectrum of 1 μ Ci Cs-137 and 1 μ Ci Co-60 laboratory sources (acquisition period: 1800 seconds)

Spectral gamma resolution data were also acquired at the MSU Calibration Facility using a unique MSU-designed thorium-232 calibration disk. The calibration disk was fabricated by MSU by spiking wet cement with a measured quantity of thorium oxide powder (thorium-232 with thorium progeny in equilibrium) to produce a 50 pCi/g standard and casting it in a mold measuring 81.3 cm in diameter by 5.1 cm thick (Figure 14).

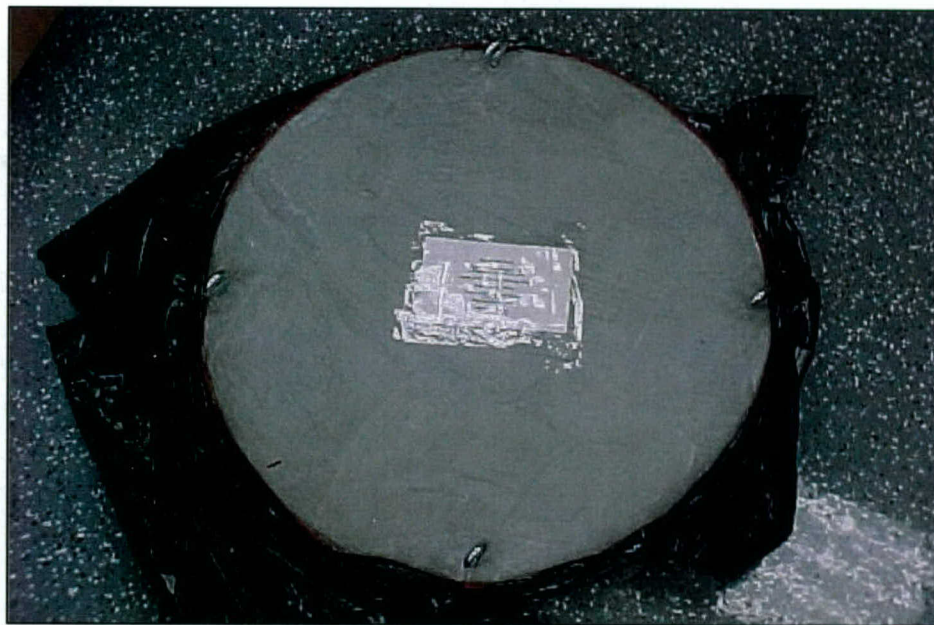


Figure 14. Calibration disk designed by Mississippi State University using thorium-232 with progeny in equilibrium (diameter 81.3 cm; thickness 5.1 cm)

The xenon gas gamma detector assembly was placed in a horizontal position approximately 10 cm above the center of the 50-pCi/g thorium calibration disk. A gamma ray spectrum of thorium-232 and thorium progeny in equilibrium was collected using the above configuration and is presented in Figure 15. The xenon gas gamma detector demonstrated the capability to fully resolve the two spectral energy lines of actinium-228, a thorium-232 progeny (daughter product), at 911 keV and 969 keV (Figure 15).

Since the two actinium-228 spectral energy lines at 911 keV and 969 keV were fully resolved in the above xenon gas spectral gamma resolution experiment, a similar laboratory experiment was conducted using a 7.62-cm (3-in.) \times 7.62-cm sodium iodide gamma detector 10 cm above the center of the MSU thorium-232 with thorium progeny calibration disk (Figure 16).

The sodium iodide gamma detector demonstrated the capability to detect the two spectral energy lines of actinium-228 but produced a smeared camel-humped peak (i.e., it was unable to separate 911 keV and 969 keV into resolved individual peaks) (Figure 17).

Additional experiments were conducted using a surrogate probe housing (i.e., placing the xenon gas gamma detector in a steel pipe with 0.64-cm wall thickness). The xenon gas gamma detector was found to provide a narrower, more defined peak (i.e., better resolution) than the peak provided by the NaI gamma detector (Figure 18).

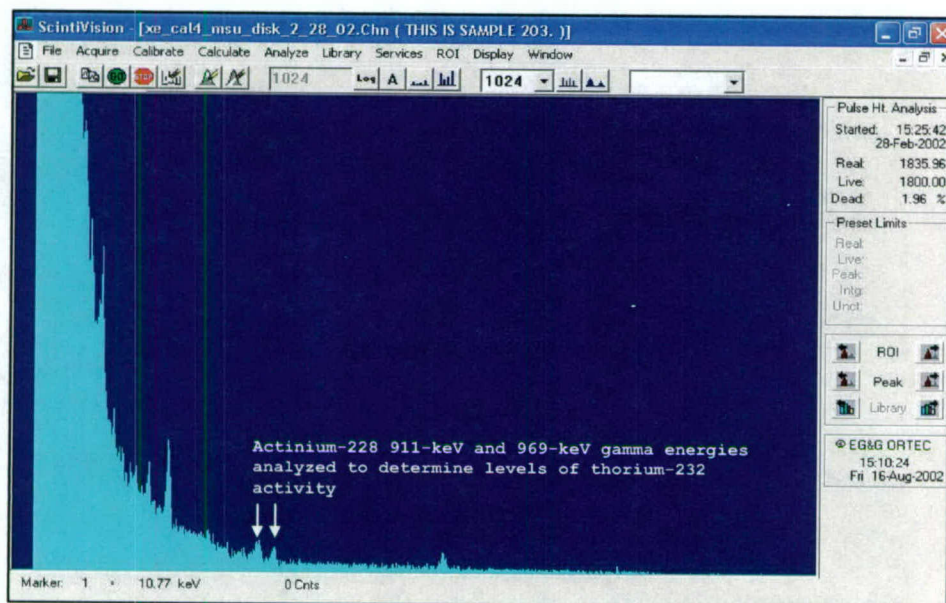


Figure 15. Xenon gas gamma detector energy spectrum collected over the Mississippi State University 50 pCi/g thorium-232 / thorium progeny calibration disk (acquisition period: 1800 seconds)

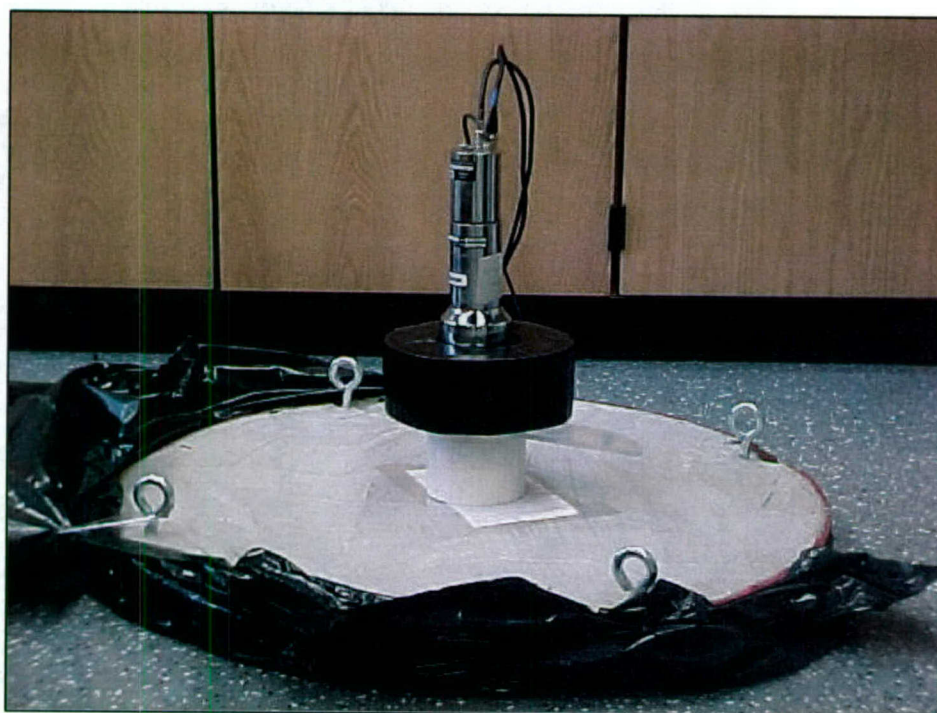


Figure 16. Sodium iodide gamma detector with lead ring positioned 10 cm above the Mississippi State University 50-pCi/g thorium-232 / thorium progeny calibration disk (acquisition period: 1800 seconds)

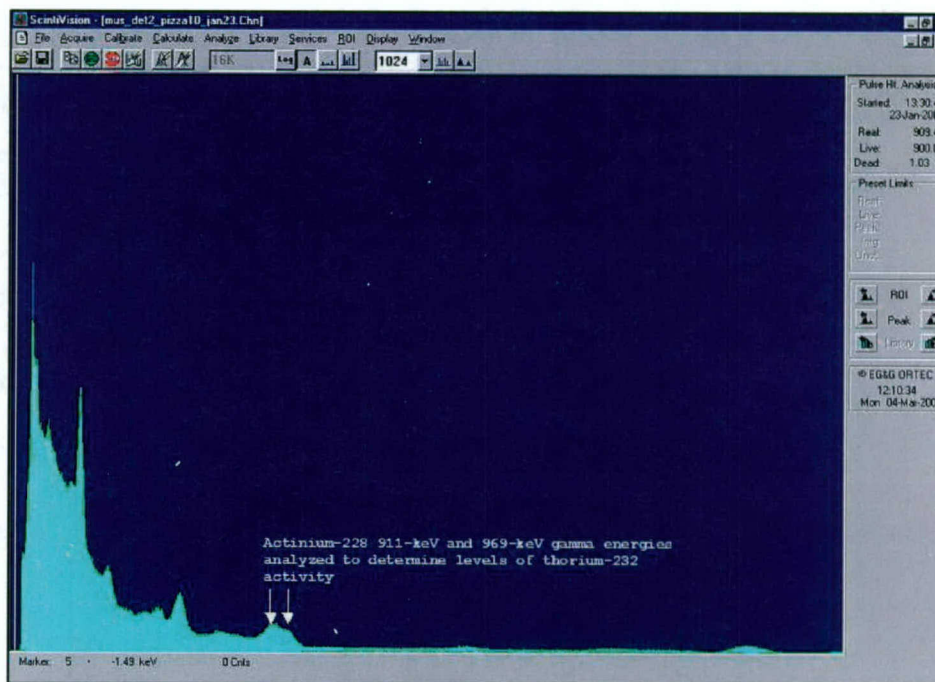


Figure 17. Sodium iodide gamma detector energy spectrum collected over the Mississippi State University 50-pCi/g thorium-232 / thorium progeny calibration disk (acquisition period: 900 seconds)

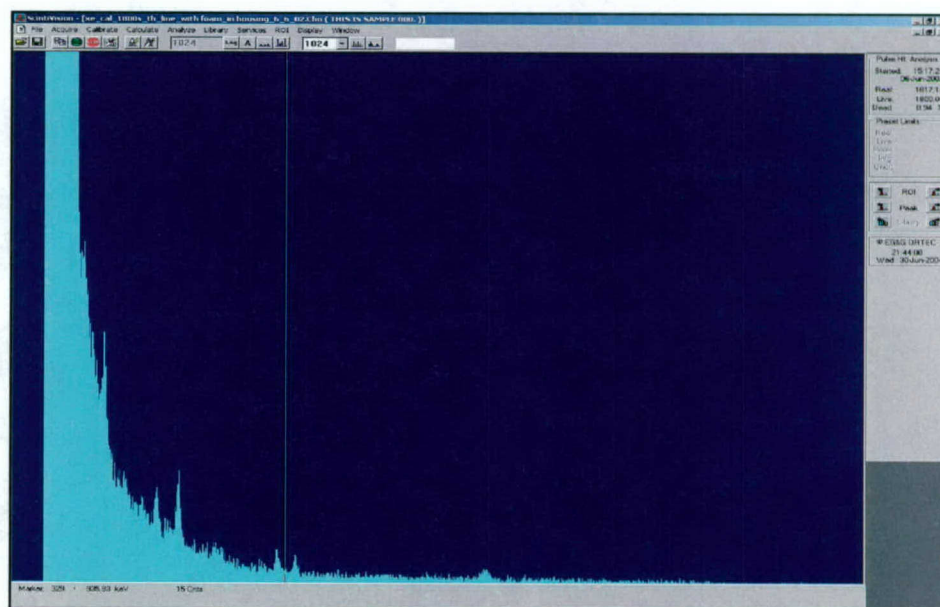


Figure 18. Xenon gas gamma detector energy spectrum collected over the Mississippi State University 50-pCi/g thorium-232 / thorium progeny calibration disk (acquisition period: 1800 seconds)

4 Xenon Probe Calibration

Calibration Isotopes

Calibration isotopes were selected to span the range of photon energies normally encountered in environmental measurements. These isotopes were also selected because their half-lives were less than a year, permitting a sequence of measurements to be made with diminishing activity. A previous study (Morgan et al. 1997) employed the same isotopes and activities, as well as the same soil. Isotopes used during calibration, their half-lives, photon energies, and production yield are shown in Table 2.

Table 2
Isotopes Used in Calibration Standard

Isotope	Half-life, days	Gamma Energy, keV	Yield, γ /dis
⁵¹ Cr	27.70	320	0.0983
⁵⁹ Fe	44.47	1099	0.565
⁵⁹ Fe	44.47	1290	0.432
⁸⁵ Sr	64.84	514	0.993
¹⁴¹ Ce	32.5	154	0.484

Calibration Media Preparation

Initial activity of each calibration isotope was 2.2 MBq on September 24, 2002. The isotopes were contained in a carrier solution of 0.1 M HCl on arrival at the MSU Radiological Sensor Calibration Facility. The isotopes were diluted with additional 0.1 M HCl on October 18, 2002. Approximately 640 mL of solution containing a mixture of all the isotopes was created in the MSU Radiological Sensor Calibration Facility. Seven batches of calibration soil were prepared by manually mixing 80 mL of calibration isotope solution into 22.72 kg of Memphis loess soil. Each batch of soil was surveyed with a NaI gamma detector to verify the uniform distribution of isotopes and placed in a large, 130.8-L polyvinyl chloride (PVC) cylinder measuring 40.6 cm in diameter and 99.1 cm tall. After the seven batches of soil were placed in the calibration cylinder, external surveys were conducted using a sodium iodide gamma detector to confirm uniform distribution of the calibration isotopes. Count rates were the same over all locations on the surface of the cylinder and thus confirmed uniformity of isotopic distribution.

within the calibration media. Because the volume of the calibration cylinder was large, the calibration media approximated an infinite medium, as would be encountered in field assessments.

Xenon Gas Spectral Gamma Probe Calibration

The xenon spectral gamma probe was inserted in the middle of the vertically standing calibration cylinder. In this configuration, the xenon spectral gamma probe was surrounded by approximately 18.3 cm of calibration medium (Figure 19).

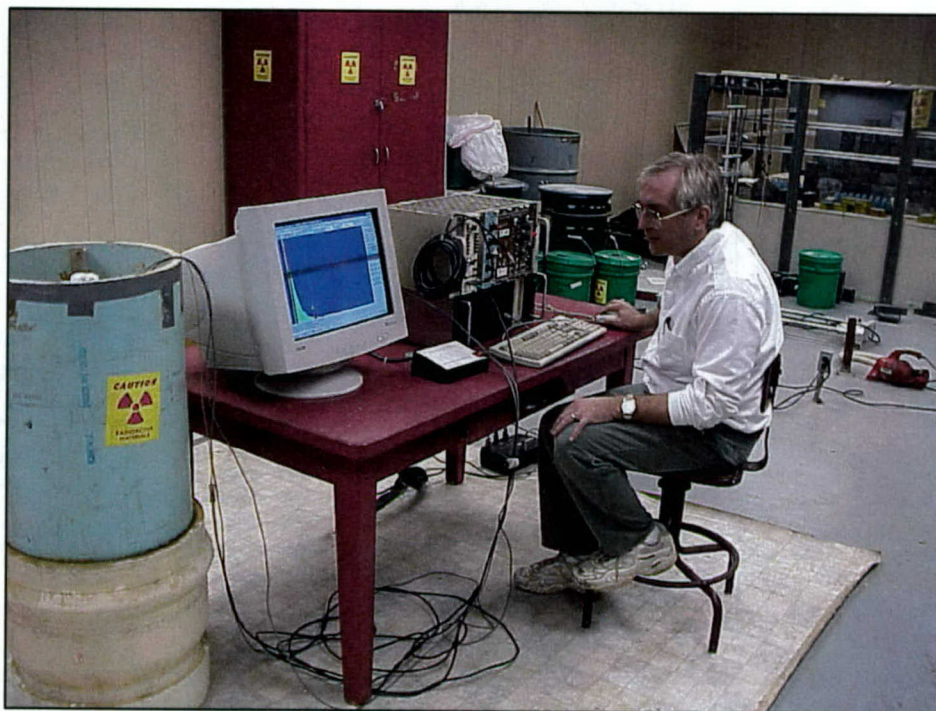


Figure 19. Xenon gas spectral gamma probe inserted in calibration medium at the Mississippi State University Radiological Sensor Calibration Facility

A series of one-hour counts was initiated. Under job control of the host computer, continuous data acquisition of spectra was established, which permitted spectra to be acquired and saved hourly throughout the entire data acquisition period, i.e., 24 spectra per day, 7 days per week, through the entire calibration period. Spectra were saved on the disk drive of the data acquisition computer and were used to document continuous operation of the xenon probe. The nuclear instrument module data acquisition and processing system is shown in Figure 20. In addition to the resolution and intrinsic efficiency, other long-term performance capabilities were documented, e.g., the minimum detectable activity as the isotopes with shorter half-lives decayed.

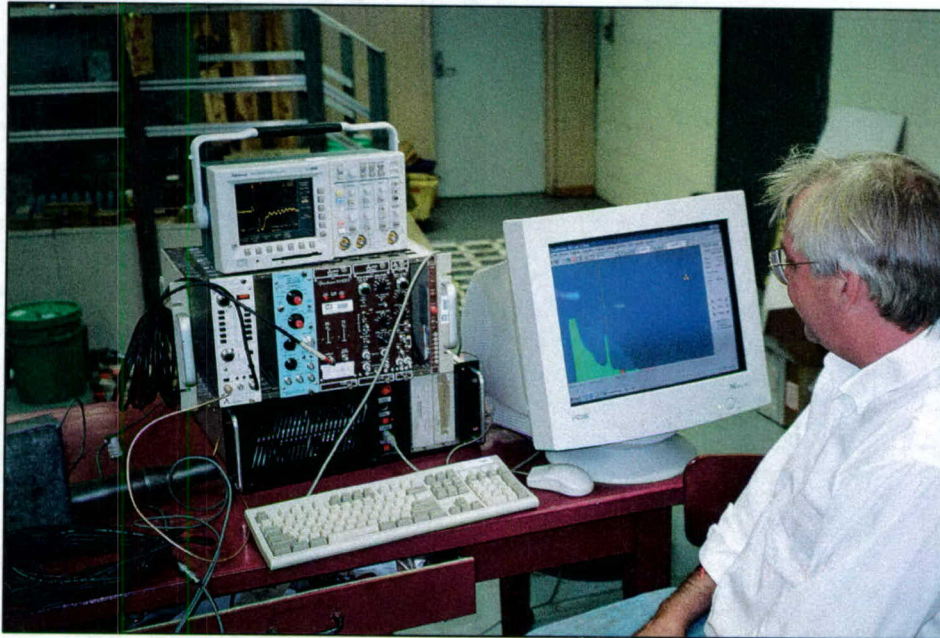


Figure 20. Nuclear instrument module data acquisition and processing system equipment used during probe calibration at the Mississippi State University Radiological Sensor Calibration Facility

Calibration Documentation

The response R to a point source attenuated through a distance x is given by the inverse square law:

$$R = S \frac{e^{-\mu x}}{4\pi r^2}$$

where

μ = the linear attenuation coefficient of the attenuating medium (cm^{-1})

r = the distance between the source and the location at which the response R is to be determined

S = the strength of the point source (photon/s)

The formula can be applied to a uniformly distributed source in a volume V . The geometry is shown in Figure 21. The point source at r is $S_V dV$, where S_V is the volumetric source strength in photon/ cm^3 -s. For cylindrical geometry, the volume element is

$$dV = \rho d\rho d\phi dz$$

where

ρ = the radial coordinate

φ = the azimuthal coordinate

z = the axial coordinate

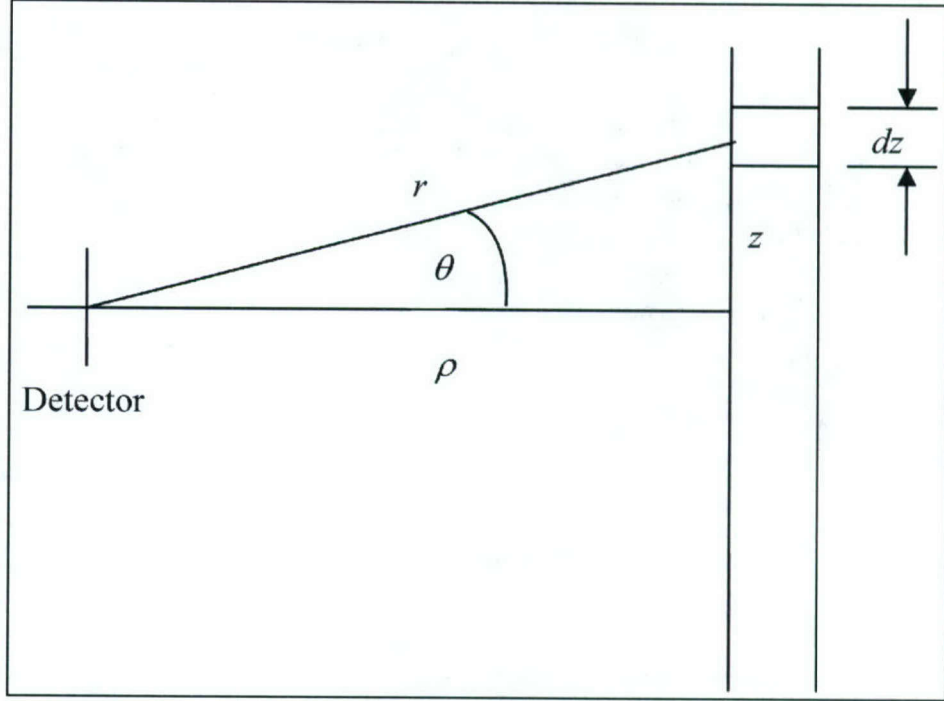


Figure 21. Geometry for distributed source

The distance r from the element of volume and the observation point is $r = \sqrt{\rho^2 + z^2}$, or $r = \rho \sec \theta$, where $\theta \equiv \tan^{-1} \frac{z}{\rho}$.

The response from an element of a uniformly distributed source is written

$$d\phi = S_v dV \frac{e^{-\mu x}}{4\pi r^2}$$

$$d\phi = S_v \frac{e^{-\mu x}}{4\pi r^2} \rho d\rho d\varphi dz$$

Integrating over azimuth, we obtain the expression

$$d\phi = S_v \frac{e^{-\mu x}}{2r^2} \rho d\rho dz$$

Now the substitution $r = \rho \sec \theta$ is made. Since $z = \rho \tan \theta$, for a given value of ρ , the differential dz becomes $dz = \rho \sec^2 \theta d\theta$.

For a detector within the cylinder along the axis, the limits of integration are

$$R_i \leq \rho < R_o$$

$$h_1 \leq z < h_2$$

where

R_i = the inner radius of the attenuating medium

R_o = the outer radius of the attenuating medium

h_1 = the lower limit of integration for the axial coordinate z

h_2 = the upper limit of integration for the axial coordinate z

If the zero for the z -axis is at the center of the cylinder, then $h_1 = -h_2$. For a detector located in the center of the cylinder containing a uniform distribution of sources, the integration may be taken from $z = 0$ to $z = h_2$, and multiplied by 2 to obtain the value for the source volume.

It is convenient to express the attenuation factor by employing the mean free path definition $b = \mu_1 t_1 + \mu_2 t_2$, where the subscripts refer to two media, in this case steel for the penetrometer and soil, and t_1 and t_2 are the distances in the respective media normal to the z -axis. Since the integration is over the source volume, it is carried out over the volume of the soil. Hence,

$$b = \mu_1 t_1 + \mu_2 (\rho - R_i)$$

The integral for number flux ϕ is then expressed by the equation

$$\phi = 2 \left[\frac{S_V}{2} \int_{\rho=R_i}^{\rho=R_o} \int_{z=0}^{z=h_2} \frac{e^{-b \sec \theta}}{(\rho \sec \theta)^2} \rho dz d\rho \right]$$

Making the substitution $dz = \rho \sec^2 \theta d\theta$, the flux becomes

$$\phi = S_V \int_{\rho=R_i}^{\rho=R_o} \left[\int_{\theta=0}^{\theta=\theta_1} e^{-b \sec \theta} d\theta \right] dz$$

$$\text{where } \theta_1 \equiv \tan^{-1} \frac{h_1}{\rho}.$$

A spreadsheet-based scheme yields an approximate value using the numerical approximation

$$\phi = S_V \int_{\rho=R_i}^{\rho=R_o} \left[\int_{\theta=0}^{\theta=\theta_1} e^{-b \sec \theta} d\theta \right] dz \approx \sum_{i=1}^{N_z} \left[\sum_{j=1}^{N_\theta} e^{-b \sec \theta_j} \Delta \theta_j \right] \Delta z_i$$

For the calibration cylinder, the number of subintervals N_z and N_θ , along the z - and θ -coordinates, respectively, are each taken to be 30.

It is desired to obtain the value that an infinite soil medium would yield. An approximate value can be obtained by increasing h_1 and R_1 until a limiting value of the integral is found. The calibration result from the finite medium can be multiplied by the ratio of infinite-medium integral to finite-medium integral to obtain the calibration factor for an infinite medium.

It is necessary to obtain the calibration factor as a function of energy. Five energies are available from the isotopes distributed in the soil.

Correction for semi-infinite medium

When the detector is deployed in the field, the response is attributable to photons originating from any location. The flux at the detector location is then approximated by extending the radius to ∞ . When this is done, the integral value changes.

Calculation of calibration coefficient

If a radionuclide is uniformly distributed over a region of indefinite extent, the uncollided flux at a point from this distribution is given by

$$\phi = S_V \int_{R_0}^{\infty} \frac{1}{\rho} \left(\int_{\theta_1}^{\theta_2} e^{-b \sec \theta} d\theta \right) d\rho$$

where

$$\phi = \text{uncollided flux, } \frac{\text{photon}}{\text{cm}^2 - \text{s}}$$

$$\rho = \text{radial coordinate, cm}$$

$$b = \text{mean free path parameter, dimensionless}$$

$$\theta = \text{angular coordinate, } \theta = \tan^{-1} \left(\frac{z}{\rho} \right), \text{ radians}$$

$$S_V = \text{volumetric photon production rate, } \frac{\text{photon}}{\text{cm}^3 - \text{s}}$$

S_V is determined from the equation

$$S_V = \tilde{S}_{V0} e^{-\lambda t} y$$

where

$$\tilde{S}_{V0} = \text{volumetric activity, } \frac{\text{dis}}{\text{cm}^3 - \text{s}}$$

$$\lambda = \text{decay constant of radionuclide, s}^{-1}$$

$$t = \text{time since calibration, s}$$

$$y = \text{photon yield, } \frac{\text{photon}}{\text{dis}}$$

This expression permits the definition of a calibration factor relating interaction rate to volumetric source strength. The interaction rate within the detector is proportional to the flux ϕ . The flux ϕ is proportional to S_V . Therefore, the interaction rate is proportional to S_V . Define the calibration factor $(CF)_F$ by the equation

$$S_{VF} = (CF)_F (\text{Count Rate})_F$$

where the subscript F denotes a finite medium. The volumetric source strength in a finite medium is determined by multiplying the count rate by the calibration factor $(CF)_F$. For the calibration cylinder, the calibration factors have been determined using spectra taken at various times.

For field applications, it is necessary to determine the calibration factor $(CF)_\infty$, which relates the count rate from a detector in a medium of infinite radial extent. The equation is similar to that for the finite medium:

$$S_{V\infty} = (CF)_\infty (\text{Count Rate})_\infty$$

where the subscript ∞ denotes the semi-infinite medium such as the ground at a site.

Let $I(H, R)$ denote the spatial integral for a finite medium. That is,

$$I(H, R) = \int_{\rho=R_1}^{\rho=R} \left[\int_{\theta=0}^{\theta=\theta_1} e^{-b \sec \theta} d\theta \right] dz$$

For an infinite medium the spatial integral may likewise be denoted by $I(H, \infty)$, defined by

$$I(H, \infty) = \int_{\rho=R_1}^{\rho=\infty} \left[\int_{\theta=0}^{\theta=\theta_1} e^{-b \sec \theta} d\theta \right] dz$$

If we examine the semi-infinite medium in which the spatial contribution is $I(H, \infty)$ and in which the source strength distribution S_{V0} exists, the flux is represented by

$$\phi_\infty = S_{V0} I(H, \infty)$$

The finite medium flux for the same volumetric source strength is

$$\phi_F = S_{V0} I(H, R)$$

The count rate, and the integral of the count rate over a specified period, is proportional to the uncollided flux:

$$(CR)_F = K\phi_F \quad \text{and}$$

$$(CR)_\infty = K\phi_\infty$$

Substituting in the analytic equations for flux,

$$\frac{(CR)_\infty}{K} = S_{V0} I(H, \infty)$$

and

$$\frac{(CR)_F}{K} = S_{V0} I(H, R)$$

Since the volumetric source strength is proportional to the calibration factor,

$$\frac{(CR)_\infty}{K} = (CF)_\infty \frac{(CR)_\infty}{K} I(H, \infty)$$

and

$$\frac{(CR)_F}{K} = (CF)_F \frac{(CR)_F}{K} I(H, R)$$

Taking the ratio of these equations,

$$\frac{(CF)_\infty I(H, \infty)}{(CF)_F I(H, R)} = 1, \quad \text{whence}$$

$$(CF)_\infty = (CF)_F \frac{I(H, R)}{I(H, \infty)}$$

The ratio was calculated using the double numerical integration scheme. Integrations were performed for five photon energies. The ratios of the infinite-medium spatial integrals to the finite-medium integrals are shown in Table 3 and verify that the calibration medium volume was appropriate.

Table 3
Calibration Coefficient Ratios

Photon Energy (MeV)	b_1	$\mu \text{ (cm}^{-1}\text{)}$	$I(H, R_1)$	$I(H, \infty)$	$\frac{I(H, R_1)}{I(H, \infty)}$
0.145	1.06	0.204	0.242874	0.2438	1.004
0.320	0.53	0.151	0.562403	0.5681	1.010
0.514	0.41	0.124	0.732451	0.7455	1.018
1.099	0.29	0.0876	1.018923	1.0596	1.040
1.292	0.26	0.0812	1.09845	1.1492	1.046

Table 4 provides the calibration factor $(CF)_F$ for the finite cylinder used in the measurement and the calculated calibration factor $(CF)_\infty$.

Table 4 Calibration Factor Summary		
Energy (MeV)	$(CF)_F$	$(CF)_\infty$
0.145	10.37	10.41
0.320	4.10	4.14
0.514	2.44	2.48
1.099	0.476	0.495
1.292	0.315	0.329

5 Xenon Probe/Sodium Iodide Probe Comparison

Laboratory Comparison in Calibration Media

The xenon gas spectral gamma probe and the sodium iodide spectral gamma probe were each evaluated separately in a 40.6-cm-diameter \times 99.1-cm-tall polyvinyl chloride (PVC) calibration cylinder filled with Memphis loess soil spiked with the isotopes listed in Table 2. The probes were placed vertically along the center line of the PVC cylinder with approximately 18.3 cm of Memphis loess soil with uniformly distributed isotopes surrounding the probes.

The xenon probe, as described in Chapter 2, was fabricated with a 6.033-cm outside diameter, 0.64-cm-thick steel wall probe housing. The xenon gas gamma detector/preamplifier assembly was installed in the center of the steel probe and consisted of a small-diameter, stainless steel, sealed 4.06-cm \times 10.16-cm cylindrically shaped gas chamber (active volume). The high-purity xenon gas acted as an ionization medium that reacted when gamma ray energy entered the high-pressure gas chamber.

The sodium iodide probe was fabricated with a 4.45-cm outside diameter, 0.64-cm-thick steel wall probe housing. The NaI gamma detector/photomultiplier tube assembly was installed in the center of the steel probe and consisted of a small-diameter, stainless steel, sealed, 1.91-cm \times 10.16-cm NaI crystal detector (active volume).

Twelve 3600-second spectral gamma data sets were collected (six with the sodium iodide spectral gamma probe and six with the xenon gas spectral gamma probe). The gamma energy peaks for each isotope were analyzed to determine areas under the peaks. The resolution of each probe was calculated by dividing the full width at half maximum taken from the energy spectrum by the photon energy of the radionuclide gamma ray. The resolutions of the sodium iodide and xenon gas spectral gamma probes were determined for the 514-keV gamma of strontium-85. The resolution of the sodium iodide spectral gamma probe was 9.8 percent (Figure 22), and the resolution of the xenon gas spectral gamma probe was 3.1 percent (Figure 23).

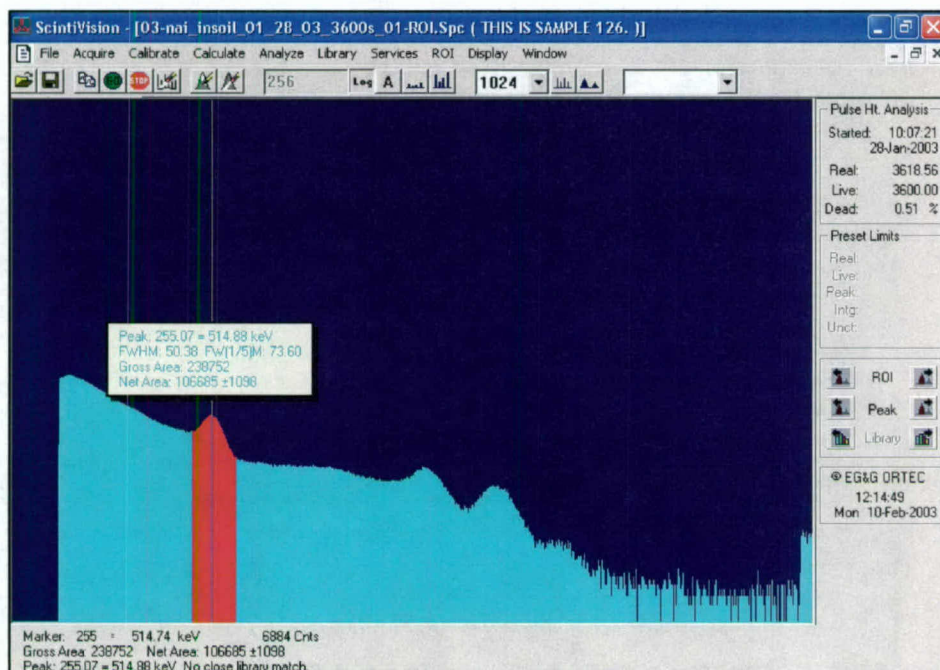


Figure 22. Sodium iodide spectral gamma probe logarithmic energy spectrum collected with the probe surrounded by 18.3 cm of radioisotope-spiked soil medium. Mississippi State University Radiological Calibration Facility (acquisition period: 3600 seconds)

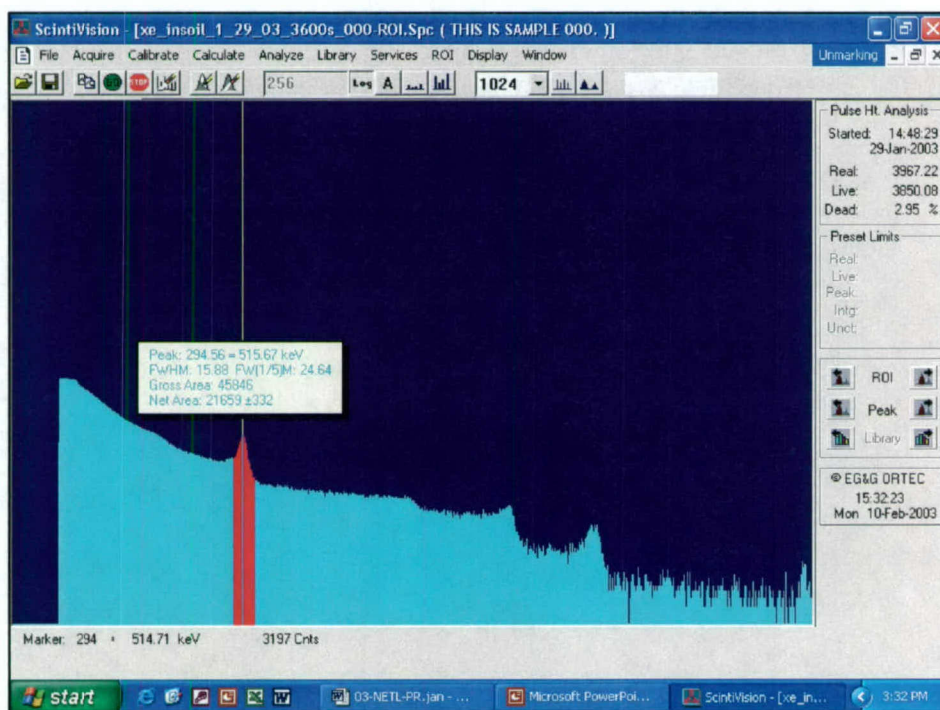


Figure 23. Xenon gas spectral gamma probe logarithmic energy spectrum collected with the probe surrounded by 18.3 cm of radioisotope-spiked soil medium. Mississippi State University Radiological Calibration Facility (acquisition period: 3600 seconds)

The concentration of each isotope in the soil mixture was calculated based on the concentration of the initial mixture and the known half-life of each isotope. The soil matrix, prepared as described in Chapter 4, had an initial activity of 2.2 MBq for each isotope present at the creation of the solution on September 24, 2002. Since the levels of radioactivity (concentration) of these isotopes decay continuously after creation, it is necessary to calculate the activity level at the time the measurements were made. Table 5 shows the half-life, energy, and corrected isotopic level of activity calculated for the matrix at the time that spectra were acquired. In addition Table 5 contains the counts obtained by analysis of the Xe and NaI spectra.

Table 5
Calculated Xe and NaI Areas and Isotope Concentrations

Isotope	Half-life, days	Energy, keV	Matrix Conc., pCi/g	Xe, cts	NaI, cts
⁵¹ Cr	27.70	320	1.3	1,953	959
⁵⁹ Fe	44.47	1,099	25.2	1,366	14,595
⁵⁹ Fe	44.47	1,290	19.3	901	9,417
⁸⁵ Sr	64.84	514	82.0	28,995	119,880
¹⁴¹ Ce	32.50	154	10.5	No Peak	No Peak

Resolution Verification

The resolutions of the xenon gas and sodium iodide spectral gamma probes were determined in the laboratory by placing 1 μ Ci Cs-137 and cobalt-60 laboratory calibration sources equidistant from the probes. In this configuration, spectral gamma data were collected using the xenon gas and sodium iodide gamma probes for 1800 seconds, and the 662-keV spectral energy peak of Cs-137 was analyzed for resolution verification. The xenon spectral gamma probe was found to provide 2.1 percent resolution (Figure 24), while the sodium iodide spectral gamma probe was found to provide 8.5 percent resolution (Figure 25) for the 662-keV spectral energy peak of CS-137.

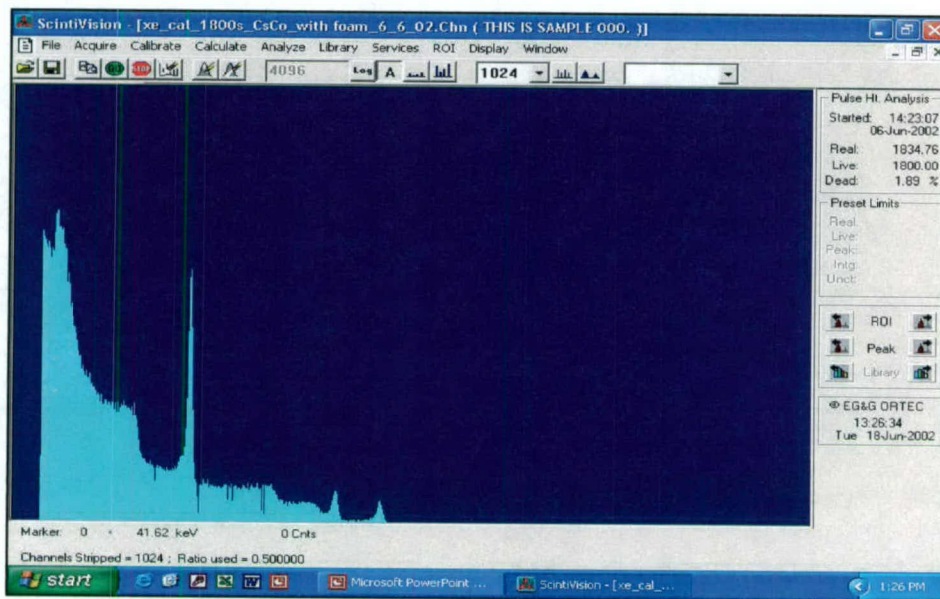


Figure 24. Xenon gas spectral gamma probe energy spectrum for 1 μ Ci Cs-137 and 1 μ Ci cobalt-60 laboratory sources; resolution for the Cs-137 662-keV spectral energy peak was 2.1 percent; acquisition period: 1800 seconds

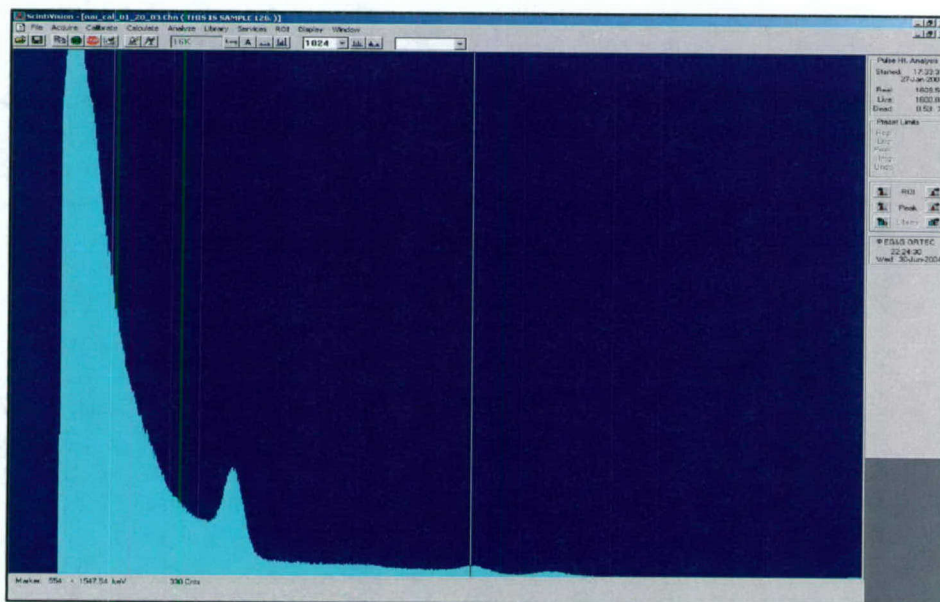


Figure 25. Sodium iodide spectral gamma probe energy spectrum for 1 μ Ci Cs-137 and 1 μ Ci cobalt-60 laboratory calibration sources; resolution for the Cs-137 662-keV spectral energy peak was 8.5 percent; acquisition period: 1800 seconds

6 Functionality Field Demonstration

Pre-demonstration Field Evaluation

The spectral gamma probe system was installed in the SCAPS truck prior to the field demonstration during late July 2003 and evaluated for functionality and anomalous behavior. It was during these evaluation tests that the xenon gas gamma detector was found to function properly for a period of time and then to generate anomalous data. The manufacturer, after reviewing the data, hypothesized that this was caused by high-voltage leakage and that the most likely cause was moisture from the high humidity (80–95 percent) experienced during the test period at the ERDC facility. The detector was removed from the system and baked for approximately 4 hours at 150°F. It functioned properly upon being reinstalled in the system. Anhydrous packing material was placed in the probe adjacent to the xenon gas detector/preamplifier module. The spectral response shown in Figure 26 is representative of system data collected after this procedure was performed.

Functionality Demonstration Site Configuration

The SCAPS high-pressure xenon gas spectral gamma probe was evaluated during a field demonstration at the ERDC facility in Vicksburg, Mississippi. The ERDC SCAPS 20-ton truck was used to push a probe into the soil to a depth of approximately 5 meters. The probe was retracted, leaving an open penetrometer hole. The SCAPS truck was backed away from the push location to facilitate the insertion of a 1.52-m-long × 5-cm-diameter polyvinyl chloride (PVC) pipe into the hole. The PVC pipe was positioned in the hole to maintain sidewall integrity of the penetrometer hole. The SCAPS truck was repositioned over the PVC pipe so that the SCAPS xenon spectral gamma probe was approximately 15 cm from the penetrometer hole. This offset in positioning was accomplished to provide a push location parallel to the penetrometer hole. Two 1 μCi sealed Cs-137 laboratory sources were attached to a nylon line and lowered in the penetrometer hole and tethered at a depth of approximately 1.5 meters. In this manner, the SCAPS xenon spectral gamma probe could be pushed parallel to the penetrometer hole and could interrogate the soil vertically for gamma activity. At a depth of 1.5 meters, the SCAPS xenon spectral gamma probe would be in position to detect and speciate Cs-137 gamma activity through approximately 15 cm of

Vicksburg loess soil. A concept drawing of the experimental field configuration is presented in Figure 27. This method of evaluation simulates the xenon spectral gamma probe detecting a point source of radioactive material in soil. Similarly, a uniform distribution of gamma-emitting radionuclides in soil will provide gamma emissions toward the probe from all directions.

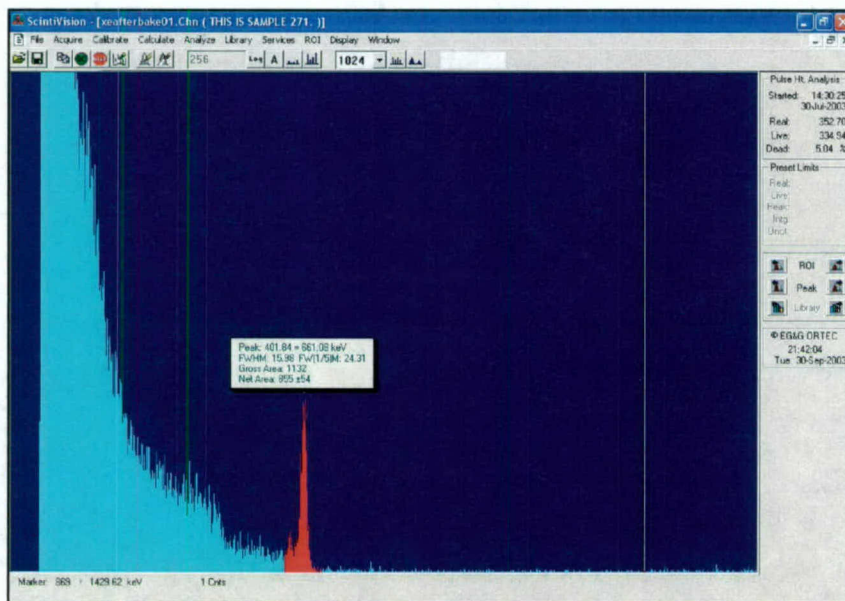


Figure 26. Cs-137 energy spectrum collected with the high-pressure xenon gas spectral gamma probe after baking

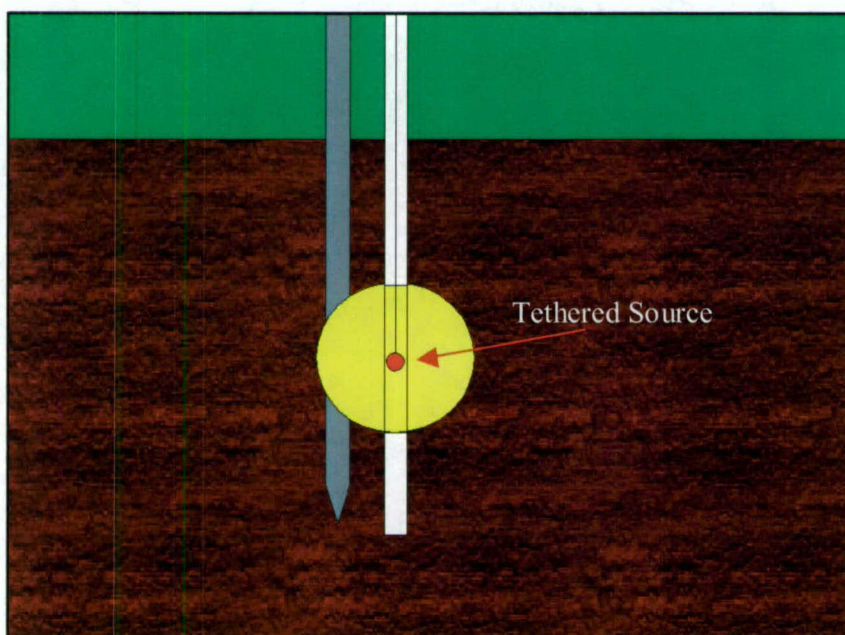


Figure 27. Functionality demonstration site configuration used to evaluate the SCAPS high-pressure xenon gas spectral gamma probe in subsurface media (the sphere represents the area of influence around the detector)

Continuous-Push Data Acquisition

The initial field evaluation was conducted to determine the capability of the xenon spectral gamma probe to detect gamma spectra and gross gamma activity during a continuous push. The data acquisition system was programmed to collect a continuous spectrum every 10 seconds of live detector time and to collect gross gamma activity in counts/second in real time as the probe was pushed into subsurface media. No discernable peak was seen during the push as the probe pushed parallel to the 2 μCi Cs-137 source tethered at approximately 1.5 m depth. Vibration attributed to the SCAPS truck engine and PTO-powered generator system was transferred via the SCAPS hydraulic clamping system into the penetrometer probe. The operation of the truck engine and PTO system during real-time continuous-push data acquisition prevented discernable gamma detection due to vibration-induced electronic noise (Figure 28).

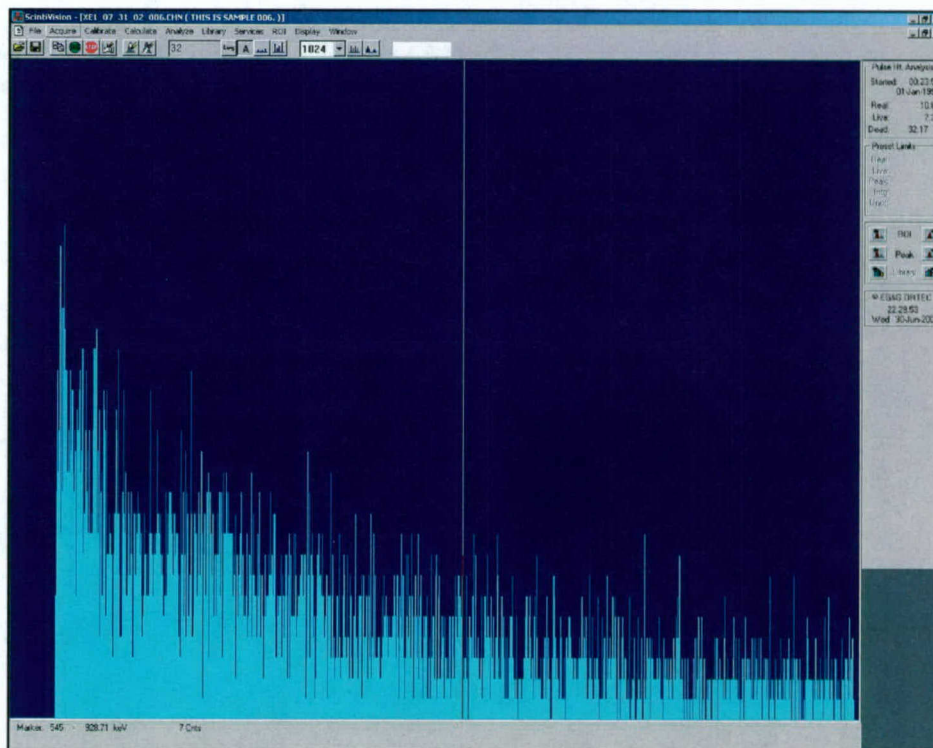


Figure 28. Continuous xenon spectral gamma probe energy spectrum collected as the probe was push parallel to the tethered Cs-137 source at approximately 1.5 m depth; acquisition period: 10 seconds

Stationary-Mode Data Acquisition

The SCAPS truck's hydraulic ram and hydraulic chuck systems were used to push the xenon gas spectral gamma probe to a selected depth for a stationary-mode interrogation of subsurface media. Various stationary modes of operation (i.e., truck/probe configurations) were investigated to determine if truck-induced vibration and the associated electronic noise could be minimized or eliminated from the xenon gas spectral gamma probe data acquisition system.

Configuration 1: Data acquisition was conducted at a depth of 1.5 m with a 2- μ Ci Cs-137 source tethered at approximately 1.5 m depth. The SCAPS truck pushed the xenon gas spectral gamma probe to the interrogation depth of 1.5 m. The SCAPS truck's hydraulic clamp was engaging the xenon gas spectral gamma probe during data acquisition. In this configuration, the SCAPS truck engine was running, and the data acquisition system was powered by the SCAPS truck's PTO-powered generator system. Electronic noise was less than the noise generated during continuous-push operations. However, leaving the probe clamped to the truck hydraulic system while the truck continued to run resulted in an unacceptable level of electronic noise (Figure 29).

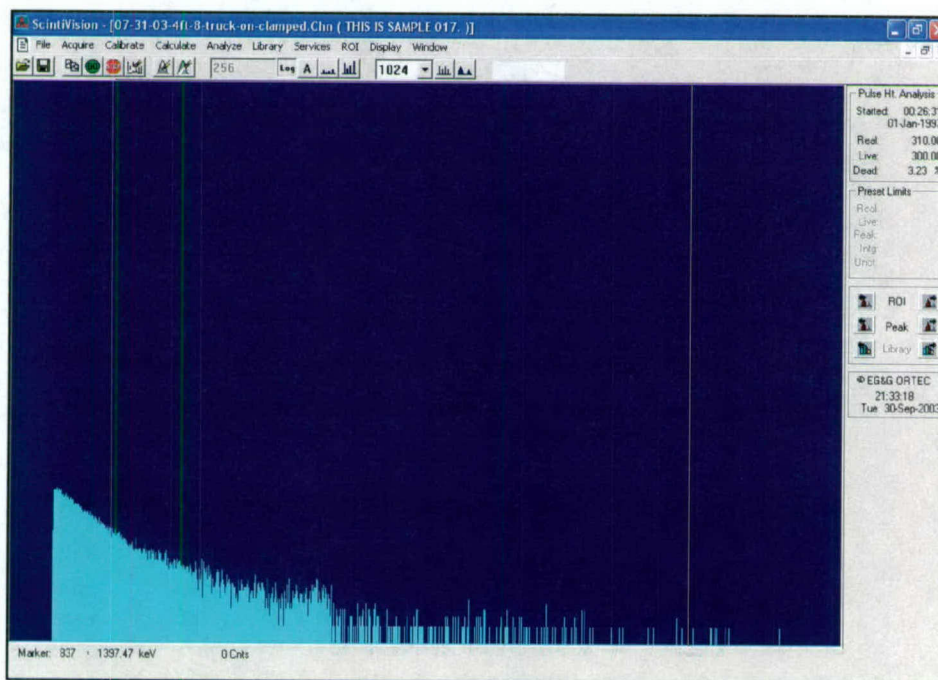


Figure 29. Xenon gas spectral gamma probe logarithmic energy spectrum of two 1- μ Ci Cs-137 sources collected at a depth of 1.5 m through 15 cm of soil; probe was in stationary-mode configuration 1; acquisition period: 300 seconds

Configuration 2a: Data acquisition was conducted at a depth of 1.5 m with a 2- μ Ci Cs-137 source tethered at approximately 1.5 m depth. The SCAPS truck pushed the xenon gas spectral gamma probe to the interrogation depth of 1.5 m. The SCAPS truck's hydraulic clamp was disengaged from the xenon gas spectral gamma probe during data acquisition. In this configuration, the SCAPS truck engine was running, and the data acquisition system was powered by the SCAPS truck's PTO-powered generator system. Electronic noise was less than the noise generated during continuous-push operations but not appreciably less than in Configuration 1. The Cs-137 gamma peak highlighted in red is better resolved than the cesium gamma peak in Figure 29. However, leaving the truck engine running during data acquisition transmitted vibration energy through the soil into the probe. Hence, configuration 2a was not acceptable for shallow subsurface interrogation depths since substantial electronic noise continued to be present in the data (Figure 30).

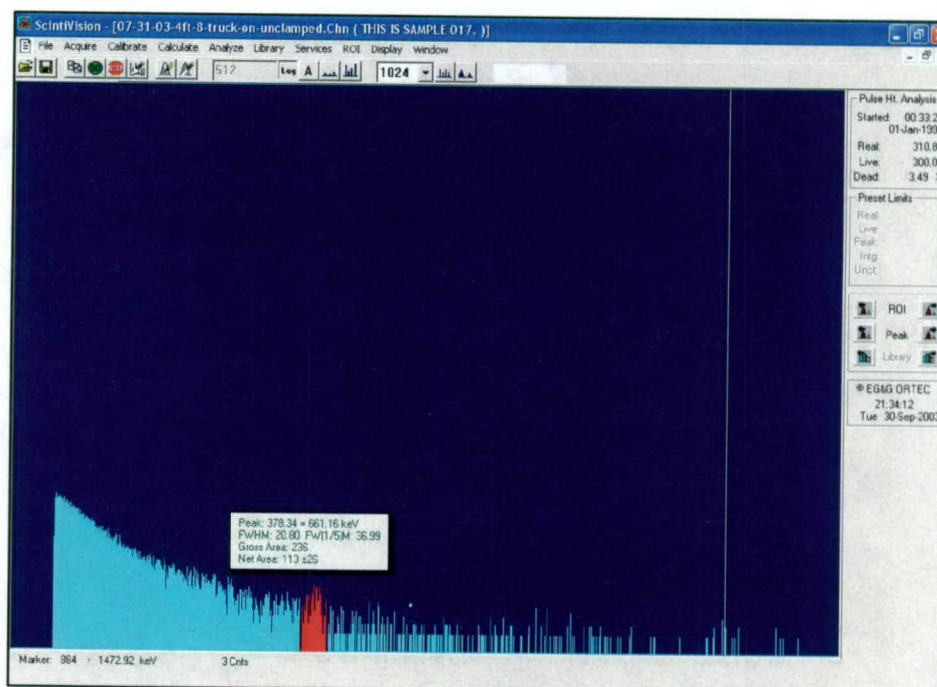


Figure 30. Xenon gas spectral gamma probe logarithmic energy spectrum of two $1\text{-}\mu\text{Ci}$ Cs-137 sources collected at a depth of 1.5 m through 15 cm of soil; probe was in stationary-mode configuration 2a; acquisition period: 300 seconds

Configuration 2b: Data acquisition was conducted at a depth of 13.71 m with a $2\text{-}\mu\text{Ci}$ Cs-137 source tethered at approximately 1.5 m depth. The SCAPS truck pushed the xenon gas spectral gamma probe to the interrogation depth of 13.71 m. The SCAPS truck's hydraulic clamp was disengaged from the xenon gas spectral gamma probe during data acquisition. In this configuration, the SCAPS truck engine was running, and the data acquisition system was powered by the SCAPS truck's PTO-powered generator system. Due to the 12.21 m of soil separating the xenon gas gamma detector from the Cs-137 source, the Cs-137 spectral gamma peak at 662 keV was not detected. However, leaving the truck engine running during data acquisition at this depth did not produce truck-vibration-induced electronic noise because the soil dampened the effects of SCAPS truck vibration. Even though no gamma activity was detectable, Configuration 3 provided an acceptable configuration for subsurface interrogations (Figure 31).

The SCAPS truck's hydraulic ram and hydraulic clamp systems were used to reposition the probe at a depth of 1.5 m. A series of configurations were evaluated to determine an optimum configuration for shallow-depth subsurface interrogations for gamma activity and radionuclide speciation.

Configuration 3: Data acquisition was conducted at a depth of 1.5 m with a $2\text{-}\mu\text{Ci}$ Cs-137 source tethered at approximately 1.5 m depth. The SCAPS truck's hydraulic clamp was disengaged from the xenon gas spectral gamma probe during data acquisition, and the SCAPS truck engine was turned off. The SCAPS data acquisition system was powered by a portable generator. Electronic noise

was negligible, and the Cs-137 gamma peak (highlighted) was resolved (Figure 32).

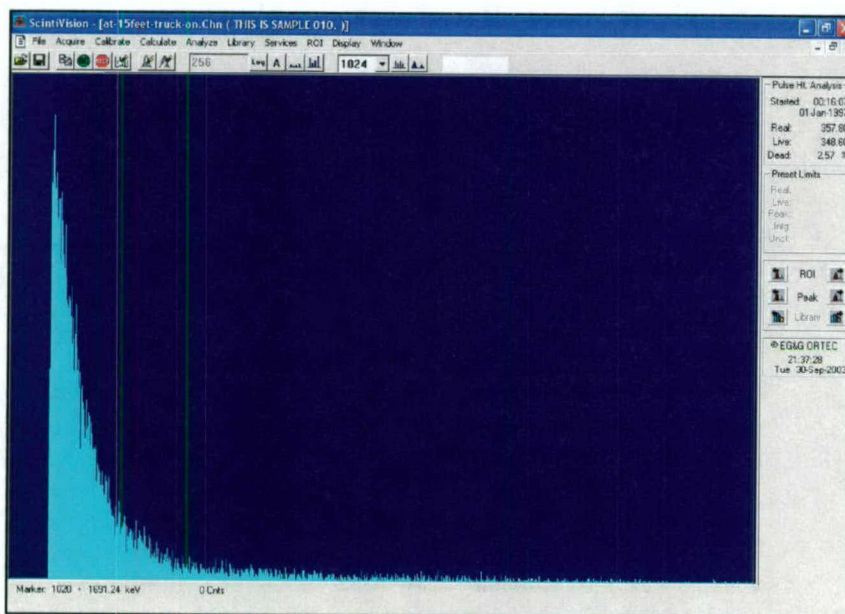


Figure 31. Xenon gas spectral gamma probe energy spectrum of clean soil acquired at a depth of 13.71 m; probe was in stationary-mode configuration 2b; acquisition period: 348.6 seconds

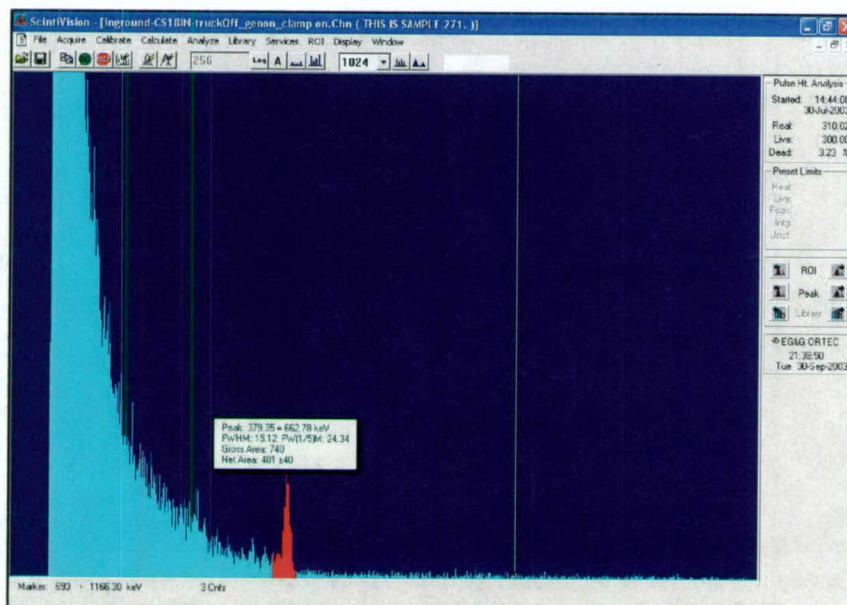


Figure 32. Xenon gas spectral gamma probe energy spectrum of two 1- μ Ci Cs-137 sources collected at a depth of 1.5 m through 15 cm of soil; probe was in stationary-mode configuration 3; acquisition period: 300 seconds

7 Conclusions

Conclusions are as follows:

- a.* ERDC successfully integrated a Mirmar-developed high-pressure xenon gas gamma detector in an ERDC-designed and -fabricated SCAPS multisensor spectral gamma penetrometer probe with soil classification sensing capabilities.
- b.* The xenon detector with an internal grid configuration was found to be sensitive to vibration during laboratory evaluation experiments. Foam material was successfully used to minimize the effects of laboratory vibration.
- c.* ERDC successfully calibrated the SCAPS xenon spectral gamma penetrometer probe at the Mississippi State University Radiological Sensor Calibration Facility. Calibration was conducted in soil media spiked with short-lived radioisotopes.
- d.* The xenon spectral gamma probe was found to provide 2.1 percent resolution for the 662-keV spectral energy line of Cs-137 versus 8.5 percent resolution for currently used sodium iodide spectral gamma probe technology.
- e.* The xenon spectral gamma probe with internal grid exhibited sensitivity to vibration and unacceptable performance during functionality field demonstration continuous-push operations and for shallow-depth interrogations when the stationary probe was attached to the SCAPS truck's hydraulic ram and chuck system.
- f.* The xenon spectral gamma probe with internal grid exhibited no sensitivity to vibration during functionality field demonstration for shallow-depth interrogations when the stationary probe was disengaged from the SCAPS truck's hydraulic ram and chuck system and powered by a portable generator.
- g.* The recommended operational mode for using the xenon spectral gamma probe with internal grid is to push the xenon spectral gamma probe to an interrogation depth and release the probe from the SCAPS truck's hydraulic ram and chuck system. In this decoupled mode, the xenon probe successfully detects and speciates (identifies) gamma-emitting radionuclides through 15 cm of subsurface soil media and provides approximately 2.1 percent resolution through the probe steel housing and soil media for Cs-137 at 662 keV. The functionality field demonstration verified that the xenon spectral gamma probe may be used for multiple interrogations at discrete depths to determine levels of subsurface radionuclide contamination.

8 Recommendations

Recommendations are as follows:

- a.* Conduct xenon spectral gamma probe subsurface interrogations for gamma energy detection and radionuclide speciation at discrete depths in a stationary decoupled mode of operation. Push the xenon spectral gamma probe to an interrogation depth and release (decouple) the probe from the SCAPS truck's hydraulic ram and chuck system to isolate the probe from truck-induced vibration.
- b.* Conduct shallow-depth xenon spectral gamma probe subsurface interrogations for gamma energy detection and radionuclide speciation in a stationary decoupled mode of operation, with the SCAPS truck engine off, and with a portable generator providing operational power.
- c.* Develop gridless xenon gas gamma detector technology to minimize the effects of vibration on detector performance and to provide the capability to detect gamma-emitting radionuclides during SCAPS continuous-probe push operations.

References

- Argonne National Laboratory. (1997). "U.S. Army Engineer Waterways Experiment Station spectral gamma probe evaluation report." Argonne National Laboratory, Environmental Research Division Internal Report, Argonne, Illinois, December 1997.
- Ballard, J. H., and Cullinane, M. J. (1998). "Innovative site characterization and analysis penetrometer system (SCAPS): In-situ sensor and sampling technologies." *Proceedings of the Symposium on the Application of Geophysics to Environmental and Engineering Problems*, Chicago, IL, 33–42.
- Ballard, J. H., Morgan, J. C., and Cullinane, M. J. (2000). "Innovative sensor technologies for radionuclide and metals speciation and quantification in situ." *Proceedings Volume of The Third International Symposium on Integrated Technical Approaches to Site Characterization*, Argonne National Laboratory, Chicago, IL, September 12–14, 2000, 65–67.
- Ballard, J. H., Morgan, J. C., and Cullinane, M. J. (2001). "Innovative technologies for in situ detection, speciation, and quantification of radionuclide and heavy metal contamination." *Proceedings CD of the Symposium on the Application of Geophysics to Engineering and Environmental Problems*, Environmental and Engineering Geophysics Society, Denver, CO, March 4–7, 2001, Paper SPT-3.
- Morgan, J. C., Adams, J. W., and Ballard, J. H. (1998). "Field use of a cone penetrometer gamma probe for radioactive waste detection." *Field Analytical Chemistry and Technology*, 2(2), 111–115.
- Morgan, J. C., Ballard, J. H., and Adams, J. W. (1997). "Field demonstration of the SCAPS cone penetrometer gamma probe for rad-waste detection." *Field analytical methods for hazardous wastes and toxic chemicals*. Air and Waste Management Association, Pittsburgh, PA, VIP-71, 600–611.

REPORT DOCUMENTATION PAGE				<i>Form Approved</i> OMB No. 0704-0188	
Public reporting burden for this collection of information is estimated to average 1 hour per response, including the time for reviewing instructions, searching existing data sources, gathering and maintaining the data needed, and completing and reviewing this collection of information. Send comments regarding this burden estimate or any other aspect of this collection of information, including suggestions for reducing this burden to Department of Defense, Washington Headquarters Services, Directorate for Information Operations and Reports (0704-0188), 1215 Jefferson Davis Highway, Suite 1204, Arlington, VA 22202-4302. Respondents should be aware that notwithstanding any other provision of law, no person shall be subject to any penalty for failing to comply with a collection of information if it does not display a currently valid OMB control number. PLEASE DO NOT RETURN YOUR FORM TO THE ABOVE ADDRESS.					
1. REPORT DATE (DD-MM-YYYY) September 2004		2. REPORT TYPE Final report		3. DATES COVERED (From - To)	
4. TITLE AND SUBTITLE Xenon Spectral Gamma Penetrometer Probe Characterization and Calibration				5a. CONTRACT NUMBER	
				5b. GRANT NUMBER	
				5c. PROGRAM ELEMENT NUMBER	
6. AUTHOR(S) John H. Ballard, Charles A. Sparrow, John C. Morgan				5d. PROJECT NUMBER	
				5e. TASK NUMBER	
				5f. WORK UNIT NUMBER	
7. PERFORMING ORGANIZATION NAME(S) AND ADDRESS(ES) Environmental Laboratory, U.S. Army Engineer Research and Development Center, 3909 Halls Ferry Road, Vicksburg, MS 39180-6199; Dave C. Swalm School of Chemical Engineering, P.O. Box 9595, Mississippi State University, Mississippi State, MS 39762-9595				8. PERFORMING ORGANIZATION REPORT NUMBER ERDC/EL TR-04-17	
9. SPONSORING / MONITORING AGENCY NAME(S) AND ADDRESS(ES) U.S. Department of Energy, National Energy Technology Laboratory, 3610 Collins Ferry Road, Morgantown, WV 26507-0880				10. SPONSOR/MONITOR'S ACRONYM(S)	
				11. SPONSOR/MONITOR'S REPORT NUMBER(S)	
12. DISTRIBUTION / AVAILABILITY STATEMENT Approved for public release; distribution is unlimited.					
13. SUPPLEMENTARY NOTES					
14. ABSTRACT Ex situ analysis to characterize subsurface media for gamma-emitting radionuclides is time-consuming and costly. A Site Characterization and Analysis Penetrometer System (SCAPS) spectral gamma penetrometer probe was designed using newly developed small-diameter high-pressure xenon gas gamma ray detector technology for the in situ speciation (identification) and quantification of subsurface gamma-emitting contaminants. This report documents the design, calibration, laboratory studies, and functionality field demonstration conducted to characterize the capabilities and limitations of the xenon spectral gamma probe. Results and comparative analysis of side-by-side simultaneous laboratory investigation/evaluation studies using SCAPS xenon spectral gamma and sodium iodine spectral gamma probes are also documented.					
15. SUBJECT TERMS Radiological site characterization SCAPS cone penetrometer			Subsurface gamma speciation and quantification in situ Xenon spectral gamma probe		
16. SECURITY CLASSIFICATION OF:			17. LIMITATION OF ABSTRACT	18. NUMBER OF PAGES 48	19a. NAME OF RESPONSIBLE PERSON
a. REPORT UNCLASSIFIED	b. ABSTRACT UNCLASSIFIED	c. THIS PAGE UNCLASSIFIED			19b. TELEPHONE NUMBER (include area code)